Seven indicators variations for multiple PV array configurations under partial shading and faulty PV conditions

Mahmoud Dhimish[1], Violeta Holmes[1], Bruce Mehrdadi[1], Mark Dales[1], Benjamin Chong[2], Li Zhang[2]
[1] School of Computing and Engineering, University of Huddersfield, United Kingdom
[2] School of Electronic and Electrical Engineering, University of Leeds, United Kingdom

Abstract

The goal of this paper is to model, compare and analyze the performance of multiple photovoltaic (PV) array configurations under various partial shading and faulty PV conditions. For this purpose, a multiple PV array configurations including series (S), parallel (P), series-parallel (SP), total-cross-tied (TCT) and bridge-linked (BL) are carried out under several partial shading conditions such as, increase or decrease in the partial shading on a row of PV modules and increase or decrease in the partial shading on a column of PV modules. Additionally, in order to test the performance of each PV configuration under faulty PV conditions, from 1 to 6 Faulty PV modules have been disconnected in each PV array configuration. Several indicators such as short circuit current (I_{sc}), current at maximum power point (I_{mpp}), open circuit voltage (V_{oc}), voltage at maximum power point (V_{mpp}), series resistance (R_s), fill factor (FF) and thermal voltage (V_{te}) have been used to compare the obtained results from each partial shading and PV faulty condition applied to the PV system. MATLAB/Simulink software is used to perform the simulation and the analysis for each examined PV array configuration.

Keywords: Multiple PV array configurations, Partial shading, Fault detection, MATLAB/Simulink

1. Introduction

Growing interest in renewable energy resources has caused the photovoltaic (PV) power market to expand rapidly. The power produced by grid-connected photovoltaic (GCPV) plants depends on various conditions such as PV module's temperature and irradiance level. Shading by the surroundings directly effects both the cell temperature and irradiance level incident on the GCPV systems [1]. There are multiple reasons for the shading affects GCPV systems. K. Lappalainen & S. Valkealahti [2] discussed the output power variations of different PV array configurations during irradiance transition caused by moving cloud. The results shows that the average rate of change in the output power during irradiance transitions is around 3%, where the maximum rate of change is approximate to 75%. Furthermore, an accurate approach method to simulate the characteristics output of a PV systems under either partial shading or mismatch conditions is proposed by J. Bai et al [3]. The method is using the analysis of the current-voltage (I-V) and power-voltage (P-V) curves for various PV systems.

A highly detailed PV array model is developed by M. Vincenzo et al [4], the PV model was developed under non-uniform irradiance conditions using PSpice. The model assumed that the PV cells temperature are homogenous for each PV module which makes the simulation and modelling of the PV system less complex. The output results shows a good agreement between the simulation model vs. outdoor experimental results. The losses associated to shading effect can be reduced by using several approaches such as the maximum power point tracking (MPPT) techniques that allow the extension of the global maximum power point. R. Yeung et al [5] proposed a global MPPT algorithm which is based on extracting the power-voltage characteristics of the PV string through varying the input power impedance.

PV array configurations which is considered in this paper is one of solutions that can significantly reduce mismatch and shading losses in GCPV plants. It is based on the PV array interconnections of PV modules which are series (S), parallel (P), series-parallel (SP), total-cross-tied (TCT) and bridge-linked (BL) and many other configurations. Several attempts were proposed by researchers to study and analyze the effect of shading on different PV array configuration in order to reduce mismatch losses and providing the maximum output power generation. These attempts can be illustrated by the following:

1. Comparison of various PV array configurations:
   F. Belhachat & C. Larbes [6] detailed a brief comparison between five different PV array configurations (S, P, SP, TCT and BL configurations). The analysis is based on MATLAB/Simulink software. The results prove that TCT configuration achieved the optimum output power performance under most shading conditions. Moreover, [7] shows a mathematical analysis of TCT PV array configuration under partial shading conditions and its comparison with other PV array configurations such as BL and honey-comb (HC) configurations. Y. Wang & P. Hsu [8] found again that in most cases TCT configuration has a superior performance over the other PV array configurations such as S, P and SP. Some other publications are based on a comprehensive review on PV array configuration under partial shading conditions such as [9 & 10].

2. New proposed PV array configuration:
   S. Pareek & R. dahiya [11] proposed a new method that allows the distribution of shading effect evenly in each PV row thereby enhance the PV array output power. The PV characteristics curves for the proposed method is much smoother than other PV array configurations such as TCT. Furthermore, B. Rani et al [12] suggested a new method for increasing the power generation from PV array configuration. In the proposed approach, the physical location of the PV modules are connected using TCT configuration, but all PV arrays are arranged based on “Su Do Ku” puzzle pattern. The performance of the system is investigated for different shading patterns and the results show that positioning the modules of the array according to “Su Do Ku” puzzle pattern yields improved performance under partially shaded conditions. However, this method faces a drawbacks due to ineffective dispersion of shade and significant increase in wiring requirements, these disadvantages of the “Su Do Ku” method have been enhanced using a new technique which is proposed by S. Potnure et al [13].

3. Power electronics techniques for enhancing PV power generation:
   B. Chong & L. Zhang [14] proposed a new controller design for integrated PV-converter modules under partial shading conditions. The control results showing rapid and stable responses are superior to that obtained by bypass diode structure which is conventionally controlled using perturbation-and-observation method. Furthermore, a new GCPV based on cascaded H-Bridge quasi-z source inverter is presented by [15], the technique is used to verify the multilevel PV interface with AC inverters to enhance the power generation of GCPV systems. E. Koutroulis & F. Blaabjerg [16] proposed a new procedure for tracking the global maximum power point of PV arrays operating under partial shading conditions using D-flip/flop and analog/digital converter strategy. Additionally, a brief comprehensive maximum power point extraction using genetic algorithm is shown in [17].

4. PV fault detection algorithms:
   There are various methods used to detect faults in GCPV plants. Some of these methods use statistical analysis techniques such as t-test [18 & 19] and standard deviation limits [20].

Furthermore, machine learning techniques have been also applied in PV systems for fault detection purposes. ANN network was used by [21] for detection multiple faults in a PV system such as faulty PV modules and faulty bypass diodes. S. Silvestre et al [22] proposed a new procedure for fault detection in PV systems which is based on the analysis of the voltage and current ratios for the entire GCPV plant.

In this work, we present a detailed modelling, comparison and data analysis for multiple PV array configurations including the series (S), parallel (P), series-parallel (SP), total-cross-tied (TCT) and bridge-linked (BL) configurations. In order to compare the performance for each PV array configuration, various partial shading and faulty PV conditions have been tested. Several indicators such as short circuit current (I_{sc}), current at maximum power point (I_{mpp}), open circuit voltage (V_{oc}), voltage at maximum power point (V_{mpp}), series resistance (R_s), fill factor (FF) and thermal voltage (V_{te}) have been used to compare the obtained by the tested partial shading and faulty conditions.

Fig. 1 shows the overall examined PV array configurations, tested case scenarios and all indicators used to compare the performance between each PV array configuration. As can be noticed, the partial shading conditions applied in this paper is not static, which means that the partial shading conditions are either increasing or decreasing among all PV modules. Additionally, in order to test the performance of each PV array configuration under faulty PV conditions, from 1 to 6 Faulty PV modules have been disconnected in order to compare between each PV indicator variations.

From the literature, there is a few data analysis on the indicators variations among partial shading and faulty PV conditions applied to multiple PV array configurations, therefore, the main contribution of this article is the comparison and data analysis of multiple PV array configurations using seven different indicators. The examined indicators has not been fully covered in previously published articles such as [6-10]. Additionally, this research does not only examine several partial shading conditions affecting PV systems but also the modelling and the analysis of several faulty PV conditions (In-active PV modules) affecting various PV array configurations.

This paper is organized as follows: Section 2 presents the modelling and simulation for one PV module using MATLAB/Simulink software. Section 3 describes the calculation of the diagnostic indicators, while section 4 illustrates the simulation, modelling and data analysis of the examined PV array configurations. Finally, section 5 and section 6 describes the discussion and the conclusion respectively.

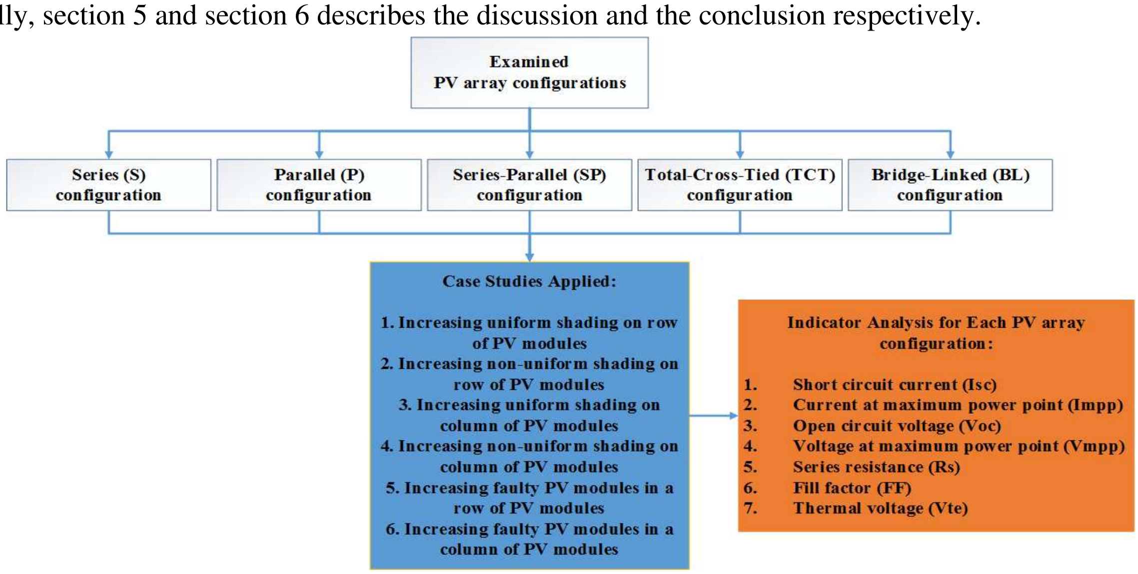

Fig. 1. All Listed PV Array Configurations Compared in this Paper, Tested Case Studies and All Indicators Used to Compare the Performance of Each PV Array Configuration

2. *Modelling and simulation of one PV module*

In this work, MATLAB/Simulink software is used to model, simulate and analyze the performance of the examined PV modules. Fig. 3(a) shows the equivalent circuit of a PV module. The voltage and the current characteristics of the PV module can be obtained using the single diode model [23] as explained in (1).

$$I = I_{ph} - I_o \left(e^{\frac{V+IR_s}{N_s V_t}} - 1 \right) - (\frac{V+IR_s}{R_{sh}}) \quad (1)$$

where I_{ph} is the photo-generated current at STC , I_o is the dark saturation current at STC, R_s is the module series resistance, R_{sh} is the panel parallel resistance, N_s is the number of series cells in the PV module and V_t is the thermal voltage and it can be calculated using (2).

$$V_t = \frac{A\,k\,T}{q} \quad (2)$$

where A the diode ideality factor, k is Boltzmann's constant, T is the module temperature in kelvin and q is the charge of the electron.

The five parameters model are determined by solving the transcendental equation (1) using Newton-Raphson algorithm [24] based only on the datasheet of the available parameters shown in Table I. The power produced by PV module in watts can be easily calculated along with the current (I) and voltage (V) that is generated by equation (1), therefore, $P_{theoretical} = IV$.

Fig 3(b) shows the PV module simulated at standard test conditions (STC):

- Irradiance 1000 W/m^2 , spectrum AM 1.5 G
- PV module temperature 25 ^oC

Using the MATLAB/Simulink software, it is possible to simulate the output voltage, current and the power of the PV module as shown in Fig. 3(c). As an example of simulation, Fig 2(a) and Fig2(b) show respectively the I-V and P-V curves of one PV module of 60 solar cells obtained with Simulink using the model described in Fig. 3(c). In this paper, the solar cell parameters used in the simulation are shown in Table1.

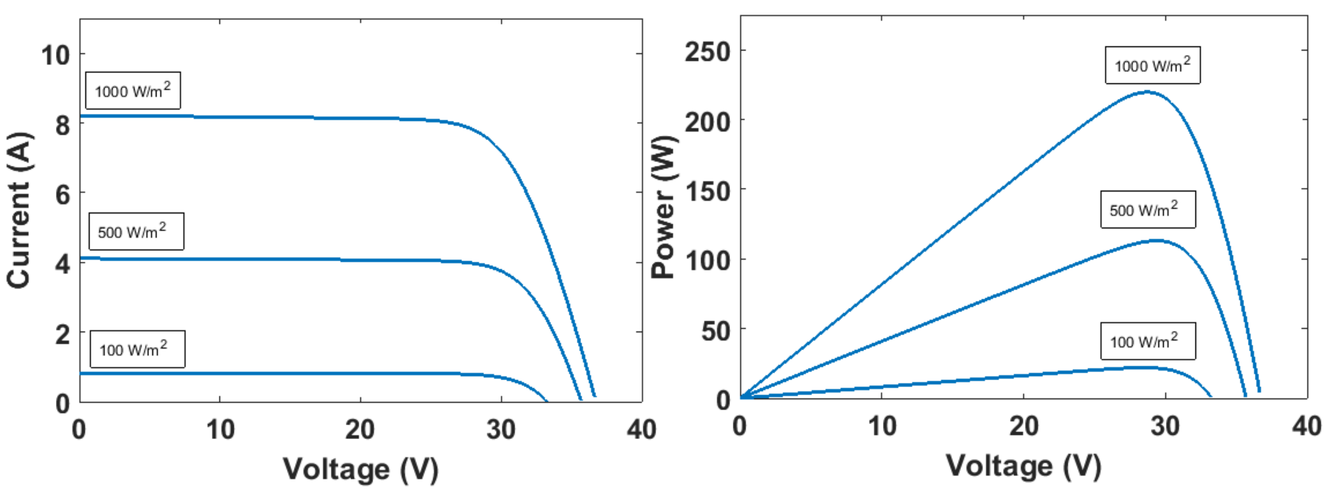

(a) (b)

Fig. 2. Simulation Results of MALTBAL/Simulink model. (a) Photovoltaic I-V Curve, (b) Photovoltaic P-V Curve

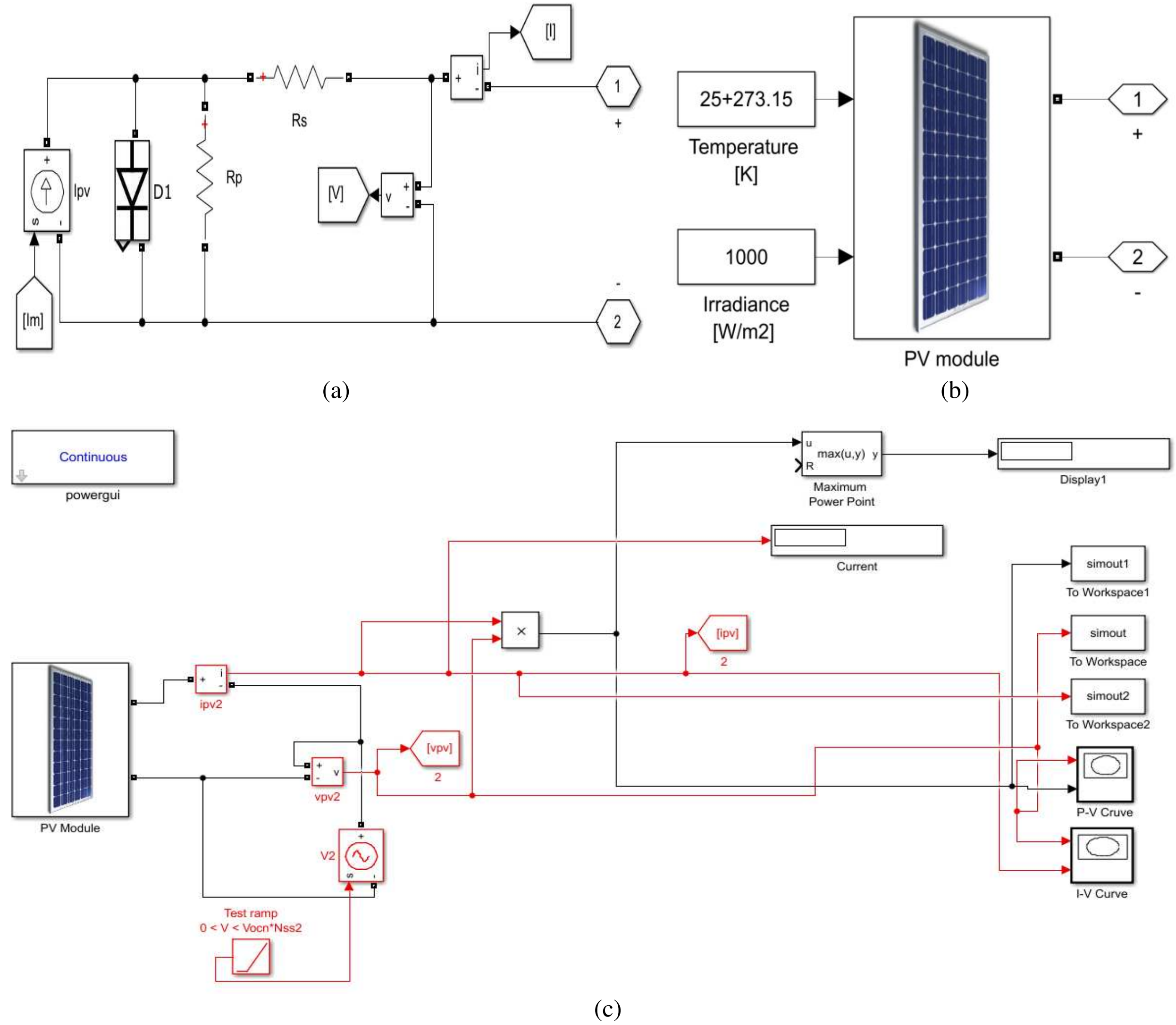

Fig. 3. Photovoltaic Modelling Using MATLAB/Simulink. (a) Equivalent Circuit of a Solar Module, (b) Simulating PV Module under STC, (c) Simulating the Output Voltage, Current and Power of the PV Module

Table 1
Electrical characteristics of SMT (60) P PV module

Solar panel electrical characteristics	Value
Peak power	220 W
Voltage at maximum power point (V_{mp})	28.7 V
Current at maximum power point (I_{mp})	7.67 A
Open circuit voltage (V_{oc})	36.74 V
Short circuit current (I_{sc})	8.24 A
Number of cells connected in series	60
Number of cells connected in parallel	1
Series resistance (R_S)	0.48484 Ω
Parallel resistance (R_{sh})	258.75 Ω
Dark saturation current (I_o)	2.8×10^{-10} A
Ideal diode factor (A)	0.9117
Boltzmann's constant (k)	1.3806×10^{-23} J.K^{-1}

3. *Calculation of the diagnostic indicators*

In order to compare the behavior of various PV array configurations. Firstly, it is required to identify the main indicators needed to investigate the change of the PV array configurations behavior. In this paper, a comparison between V_{mpp}, V_{oc}, I_{mpp}, I_{sc} and P_{mpp} have been estimated for various PV array configurations. Additionally, new diagnostic indicators have been used and briefly explained in this section.

3.1 Equivalent thermal voltage (V_{te})

In previous work [25 & 27] an estimation of the thermal voltage of a PV model under partial shading conditions has been expressed by (3).

$$V_{te} = \frac{(2V_{mp} - V_{oc})(I_{sc} - I_{mp})}{I_{mp} - (I_{sc} - I_{mp})\ln(\frac{I_{sc} - I_{mp}}{I_{sc}})} \tag{3}$$

where V_{mp} is voltage at maximum power point, I_{mp} presents the current at the maximum power point, V_{oc} is the open circuit voltage and I_{sc} is the short circuit current estimated by the I-V or P-V curve of the PV module.

A second commonly used method to estimate the thermal voltage is to evaluate the change of the diode ideality factor *A* of the PV module [26]. This method can be calculated using (4).

$$V_{te} = \frac{N_s \, A \, k \, T}{q} \tag{4}$$

where N_s is the number of solar cells connected in series, k is the Boltzmann constant, T is the junction temperature in kelvin and q is equal to the charge of an electron.

In this paper, the first method was used to estimate the thermal voltage due to its simplicity and it does not require the estimation of the ideality factor for the PV modules [18]. The estimation of the ideality factor is usually cannot be calculated using the maximum power point tracking units provided in the PV systems. However, the first method does contain all parameters which are normally available to the user of the grid-connected PV (GCPV) plants.

The estimation of V_{te} for the PV module used in this paper under various irradiance levels (100~1000 W/m^2) are shown in Fig. 4. The PV module temperature for all measurements is at STC 25 ^{o}C and the solar cell parameters used in the simulation are shown in Table1.

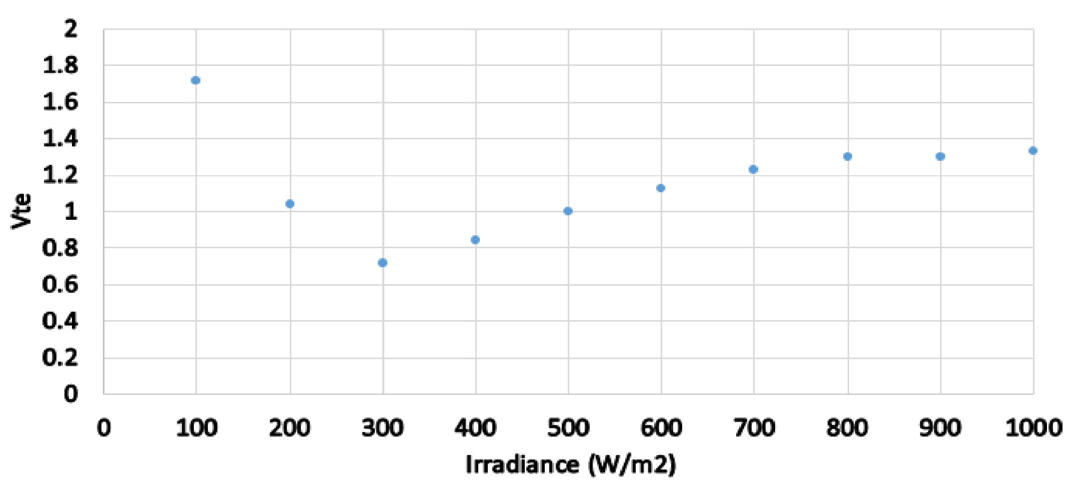

Fig. 4. Thermal Voltage Estimation under Various Irradiance Levels

3.2 Fill factor (FF)

The fill factor (FF) is a generic diagnostic indicator which is sensitive to power losses due to shading and faulty conditions occurring in PV systems [27]. FF is sufficiently robust to the irradiance change and the temperature levels. FF can be calculated using (5).

$$FF = \frac{I_{mp}\, V_{mp}}{I_{sc}\, V_{oc}} \tag{5}$$

The fill factor is a good indicator since it depends on the voltage and current changes in the PV modules. Fig. 5(a) shows the I-V curve of the PV module used in this work. Also it shows the location of the parameters used in the calculation of the FF indicator.

At STC, the PV module used in this work can be evaluated as shown in (6).

$$FF = \frac{I_{mp}\, V_{mp}}{I_{sc}\, V_{oc}} = \frac{7.67 \times 28.7}{8.18 \times 36.74} = 73.25\% \tag{6}$$

Fig. 5(b) shows the variations of the FF under various irradiance levels (100~1000 W/m^2).

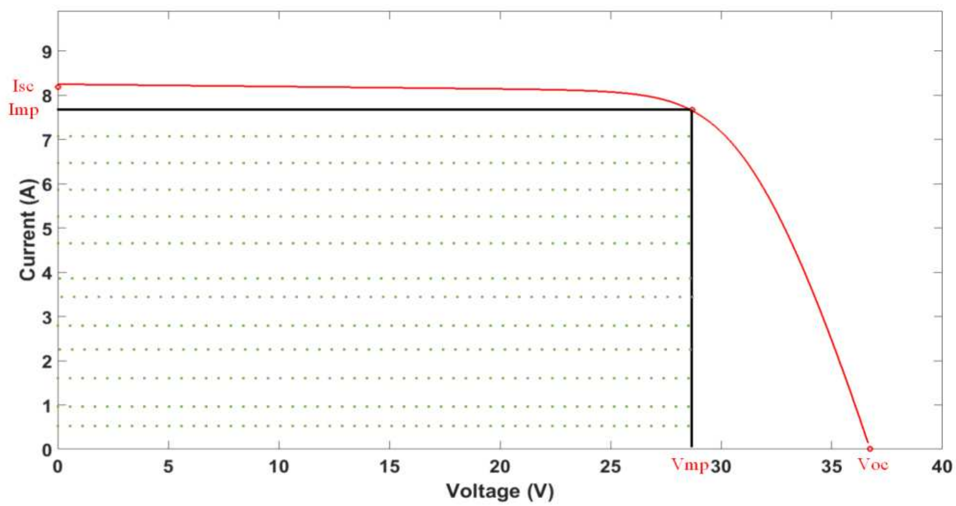

(a)

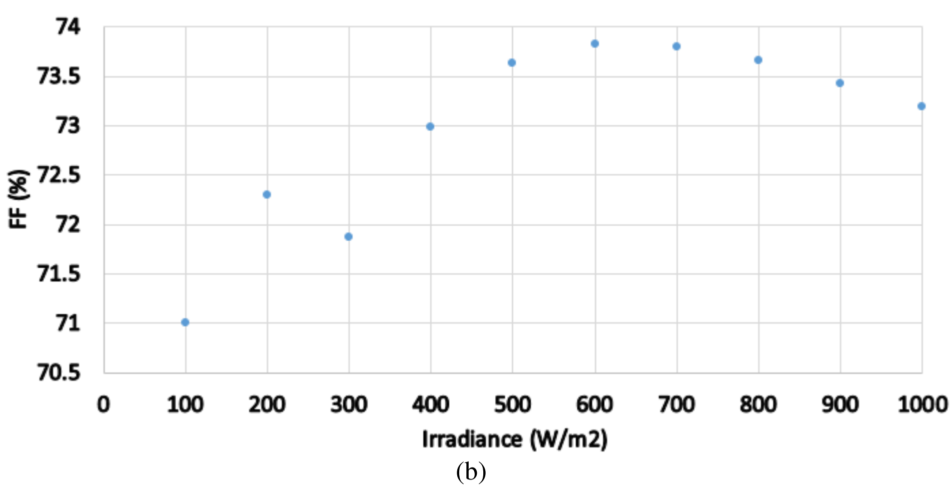

(b)

Fig. 5. (a) Fill Factor Parameters Estimation Using Photovoltaic I-V Curve, (b) Fill Factor Estimation under Various Irradiance Levels

3.3 PV series resistance (R_s)

Method 1:

One commonly used method to estimate R_s is to evaluate the derivative of the voltage with respect to the current at the V_{oc}. The final expression to approximate the series resistance is described by (7).

$$R_{s,e} = -\left.\frac{dV}{dI}\right| V \approx V_{oc} = -\left.\frac{V_2 - V_1}{I_2 - I_1}\right| V \approx V_{oc} \quad (7)$$

where V_2, V_1, I_2 and I_1 are the voltage and the current points estimated near to V_{oc}.

The value of the series resistance estimated by the derivative may vary with the irradiance the temperature conditions [28]. D. Sara et al [29] proposed a method to translate the value of the estimated R_s to STC in order to mitigate the effect of the irradiance (G) and PV module temperature (T). The expression is illustrated by (8).

$$R_s = R_{s,e} + \frac{V_{te}}{I_{sc}} \left(\frac{G}{G_{STC}} \times \frac{T_{STC}}{T} - 1\right) \quad (8)$$

where G_{STC} is equal to 1000 W/m^2 and T_{STC} is equal to 25 °C.

As can be noticed, the estimation of the series resistance requires the voltage and the current measurements of at least two point of the I-V curve close to the V_{oc}. The method also requires the value of the irradiance and the PV modules temperature to perform the estimation of the series resistance value.

Method 2:

Another method of estimating the series resistance of a PV module is to evaluate the derivative of the voltage with respect to the current at the short circuit and maximum power point, such point is characterized by a current lower, but closer to I_{mpp} and it is denominated as Q. This method was proposed by [21] and used in [27 and 28] for the estimation of R_s. There are two options to calculate Q (9 & 10).

$$Q1 = I_{sc,e} - (0.75 \times I_{mpp}) \quad (9)$$

$$Q2 = I_{sc,e} - (0.60 \times I_{mpp}) \quad (10)$$

where the value of $I_{sc,e}$ is the estimated short circuit current and can be evaluated using (11).

$$I_{sc,e} = \frac{I_{sc}}{K_1} \quad (11)$$

where K_1 is the ratio between I_{mpp} and I_{sc} and it is assumed as constant value of 0.92 as described by [21].

The final expression of estimating the value of the series resistance is expressed by (12).

$$R_s = -\left.\frac{dV}{dI}\right| I \approx Q = -\left.\frac{V_2 - V_1}{I_2 - I_1}\right| I \approx Q \quad (12)$$

The evaluation of the series resistance requires at least two points of the I-V curve for the PV module. Furthermore, it is required to measure:

1. Current at maximum power point (I_{mpp})
2. Short circuit current (I_{sc})

Fig. 6 shows the value of the series resistance estimated using method 1 and method 2. The estimated values of the R_s are compared with the measured R_s. Therefore, the difference between the measured values with the estimated values can be expressed by (13).

$$Difference = Estimated\ R_s - Measured\ R_s \tag{13}$$

Table 2 shows the comparison between the estimated R_s and measured R_s using method 1: at V_{oc}, and method 2: at Q1 and Q2. The minimum average difference is equal to 1.71% obtained for method 1. Therefore, in this paper, method 1 is used for the estimation of R_s.

Table 2
Difference between Estimated R_s and Measured R_s

Irradiance level (W/m^2)	Measured R_s (Ω)	Estimated R_s (Ω) using method 1		Estimated R_s (Ω) using method 2, Q1		Estimated R_s (Ω) using method 2, Q2	
		R_s (Ω)	Difference	R_s (Ω)	Difference	R_s (Ω)	Difference
1000	0.48484	0.512558	0.027717	0.532558	0.047718	0.582558	0.097718
900	0.537836	0.545554	0.007718	0.595554	0.057718	0.595554	0.057718
800	0.567762	0.58548	0.017718	0.62548	0.057718	0.70548	0.137718
700	0.623004	0.637755	0.014751	0.681755	0.058751	0.687755	0.064751
600	0.698996	0.706714	0.007718	0.606714	-0.09228	0.816714	0.117718
500	0.789787	0.804505	0.014718	0.837845	0.048058	0.934505	0.144718
400	0.934482	0.9522	0.017718	0.9822	0.047718	1.1322	0.197718
300	1.172762	1.20048	0.027718	1.23448	0.061718	1.31048	0.137718
200	1.688184	1.705902	0.017718	1.729902	0.041718	1.815902	0.127718
100	3.240672	3.25839	0.017718	3.28139	0.040718	3.33839	0.097718
		Average Difference (%)		Average Difference (%)		Average Difference (%)	
		1.71		3.69		11.81	

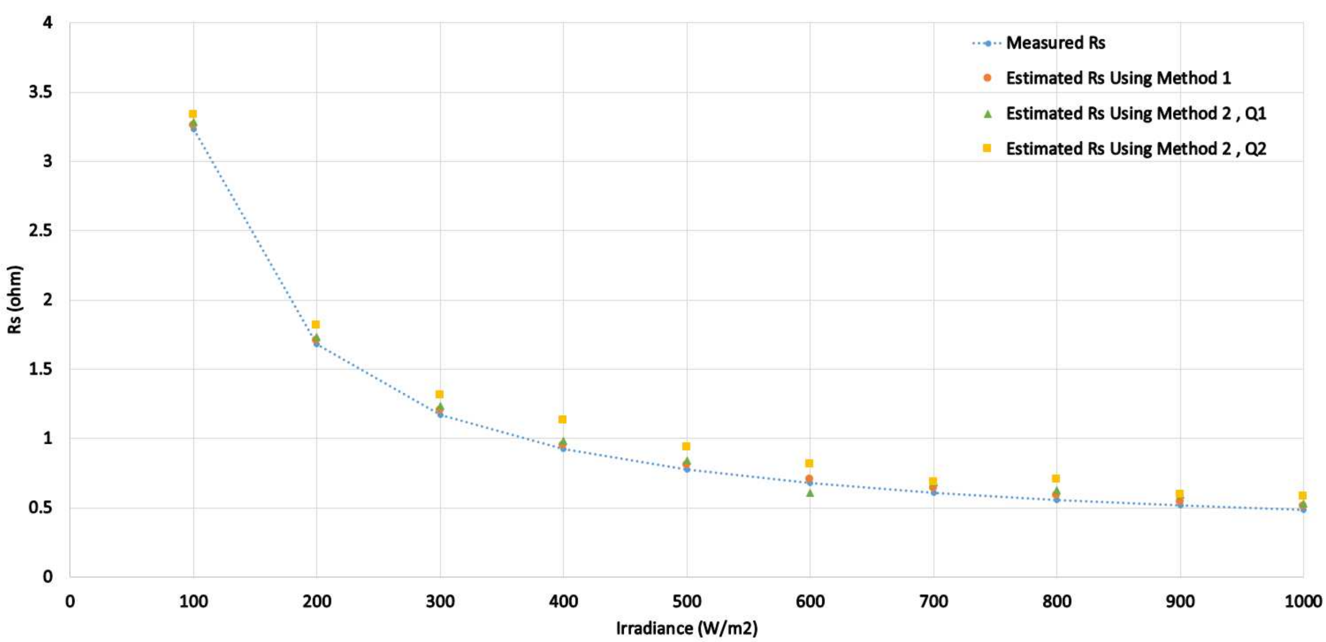

Fig. 6. Evaluating the Series Resistance of a PV Module under Various Irradiance Levels

4. Simulation, modelling and data analysis of multiple PV array configurations

The aim of this section is to present the multiple PV array configurations used in this study. In order to test the multiple PV array configurations, 24 PV modules were used. Each PV module consists of 60 PV modules connected in series and protected by bypass diodes. The PV modules temperature was fixed at the standard test condition (STC) 25 ºC.

4.1 Types of examined PV array configurations

Five common PV array configurations were used in order to examine the main indicators which are mostly changeable during the normal operation mode, partial shading and faulty PV conditions. The examined PV array configurations are listed as the following:

1. Series (S) configuration
2. Parallel (P) configuration
3. Series-Parallel (SP) configuration
4. Total-Cross-Tied (TCT) configuration
5. Bridge-Linked (BL) configuration

MATLAB/Simulink software is used to create the listed PV array configurations. Appendix A contains all MATLAB/Simulink software models which are used to configure the grid-connected PV (GCPV) systems. Furthermore, during the simulation all indicators: V_{mpp}, V_{oc}, I_{mpp}, I_{sc}, P_{mpp}, R_s, FF and V_{te} were saved in a spreadsheet to evaluate the performance of each PV array configuration separately.

4.2 PV array configurations under STC

This section presents the variations of all required indicators at standard test conditions applied to the PV array configurations. Table 3 shows the value of all indicators for the different PV array configurations. The main outcomes from the obtained results can be expressed by the following:

1. Series configuration: the dominant indicator is the value of the V_{oc}, V_{mp} and the value of the thermal voltage.
2. Parallel configuration: I_{sc}, I_{mpp} and the thermal voltage which has the least value across all PV configurations.
3. SP, TCT and BL configurations have a common similarity across all indicators.
4. At STC, the FF for all PV configurations is approximately equal to 73.2%.

From Table 4 it is possible to evaluate the value of the series resistance across one PV module in the GCPV systems according to the mathematical expressions listed below in Table 3.

Table 3
Mathematical Calculations of R_s for Various GCPV Plants

PV array configuration	Mathematical expression for estimating the value of R_s for one PV module in the PV array configuration	
S	$\frac{R_{s\,(Obtained\ from\ the\ I-V\ Curve)}}{24_{(total\ PV\ module\ in\ the\ PV\ array\ configuration)}}$	(14)
P	$R_{s\,(Obtained\ from\ the\ I-V\ Curve)} \times 24_{(total\ PV\ module\ in\ the\ PV\ array\ configuration)}$	(15)
SP, TCT and BL	$\frac{R_{s\,(Obtained\ from\ the\ I-V\ Curve)} \times 4_{\ (number\ of\ PV\ columns)}}{6_{\ (number\ of\ PV\ modules\ in\ one\ PV\ row\ "PV\ String")}}$	(16)

Table 5 shows that the estimation of the series resistance for a single PV module using the mathematical expressions listed in Table 3 at STC. There is a slightly difference between the real measured R_s values at STC with the calculated R_s using (14-16). The percentage of the average difference between the measured R_s and the calculated R_s is equal to 2.2%.

Table 4
Indicators Values Estimated for All Examined PV Array Configurations

PV configuration	I_{sc} (A)	V_{oc} (V)	I_{mpp} (A)	V_{mpp} (V)	P_{mpp} (W)	R_s (Ω)	V_{te} (V)	FF (%)
S	8.177	881.2	7.538	700.3	5279	12.18175	36.2059	73.2608
P	196.2	36.74	181.4	29.1	5279	0.020116	1.44597	73.2305
SP	32.71	220.3	30.26	174.4	5279	0.757576	8.59957	73.2353
TCT	32.71	220.3	30.33	174	5278	0.757576	8.31149	73.2363
BL	32.71	220.3	30.33	174	5278	0.757576	8.31149	73.2363

Table 5
Estimated R_s for One PV Module Only

PV configuration	R_s (Ω)	Calculated R_s for one PV module (Ω)	Measured R_s for one PV module at STC (Ω)	Difference in the estimation of R_s (%)
S	12.18175	0.507573	0.48484	2.273299
P	0.020116	0.482772	0.48484	-0.20675
SP	0.757576	0.505051	0.48484	2.021051
TCT	0.757576	0.505051	0.48484	2.021051
BL	0.757576	0.505051	0.48484	2.021051

4.3 Partial shading conditions applied to the PV array configurations

In order to evaluate the behavior of each PV configuration under non-uniform irradiance conditions and to choose the most optimal configuration that provides that highest performance and identifying the main indicators which are changing significantly in each PV configuration, two different shading scenarios and two faulty PV conditions were tested for each PV configuration under a fixed temperature 25 ^oC.

4.3.1 Scenario 1: row level

In this part, the focus will be on the performance of the PV configurations which are affected by a uniformly and non-uniform shading patterns on a row level (row of PV modules). Fig. 7 shows both patterns used to evaluate the row shading conditions effects on the PV modules.

As can be noticed from Fig. 7, two different partial shading conditions was performed. The first partial shading pattern is applied on a row of PV modules at irradiance level equal to 500 W/m^2. However, the second shading pattern consists of various irradiance levels (200, 400, 600 and 800 W/m^2) applied to four PV modules.

Fig. 8(a) shows the maximum output power obtained in each PV array configuration under shading pattern 1. The P configuration shows the maximum output power comparing to all other examined PV array configurations. The configurations S, SP, TCT and BL provide the same maximum power in each case.

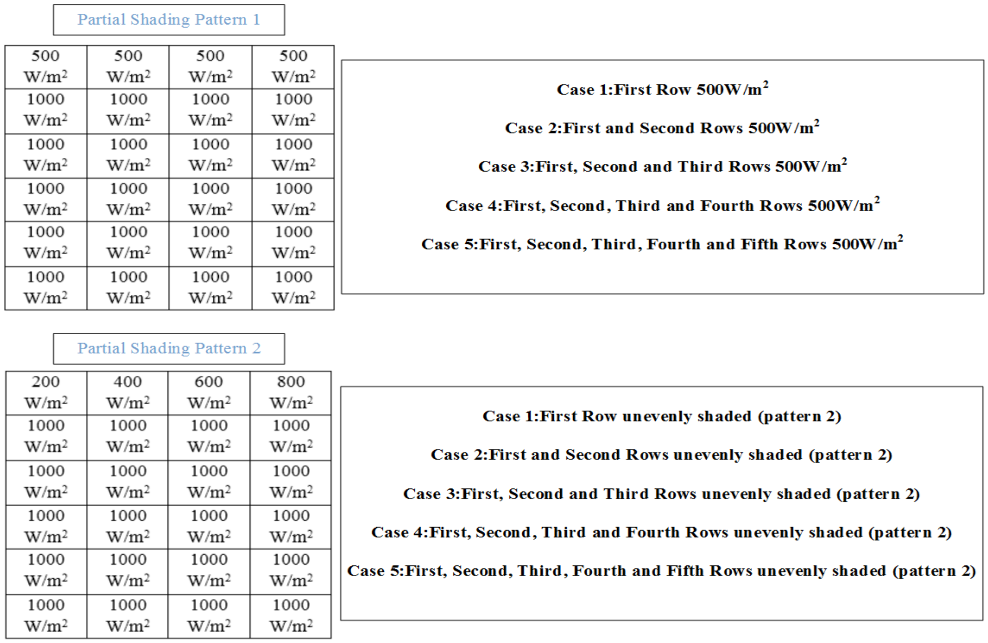

Fig. 7. Partial Shading Patterns for Scenario 1: Row Level

Fig. 8(b) proves that P configuration has the maximum output power among all other PV array configurations under shading pattern 2. TCT and BL comes second best choice whereas the series configuration has the lowest performance.

In each shading pattern, the series resistance (R_s) was estimated using method 1 which has been discussed previously in section 3.3. Table 6 shows the estimated R_s for each PV array configuration for shading pattern 1. Rs estimated for the S configuration is increased by approximate to 1.13 Ω. Additionally, the estimated series resistance for SP, TCT and BL configurations is increased by approximate to 0.07 Ω. There is a very small amount of change in the series resistance obtained for P configuration, the reduction is only equal to 0.002 Ω.

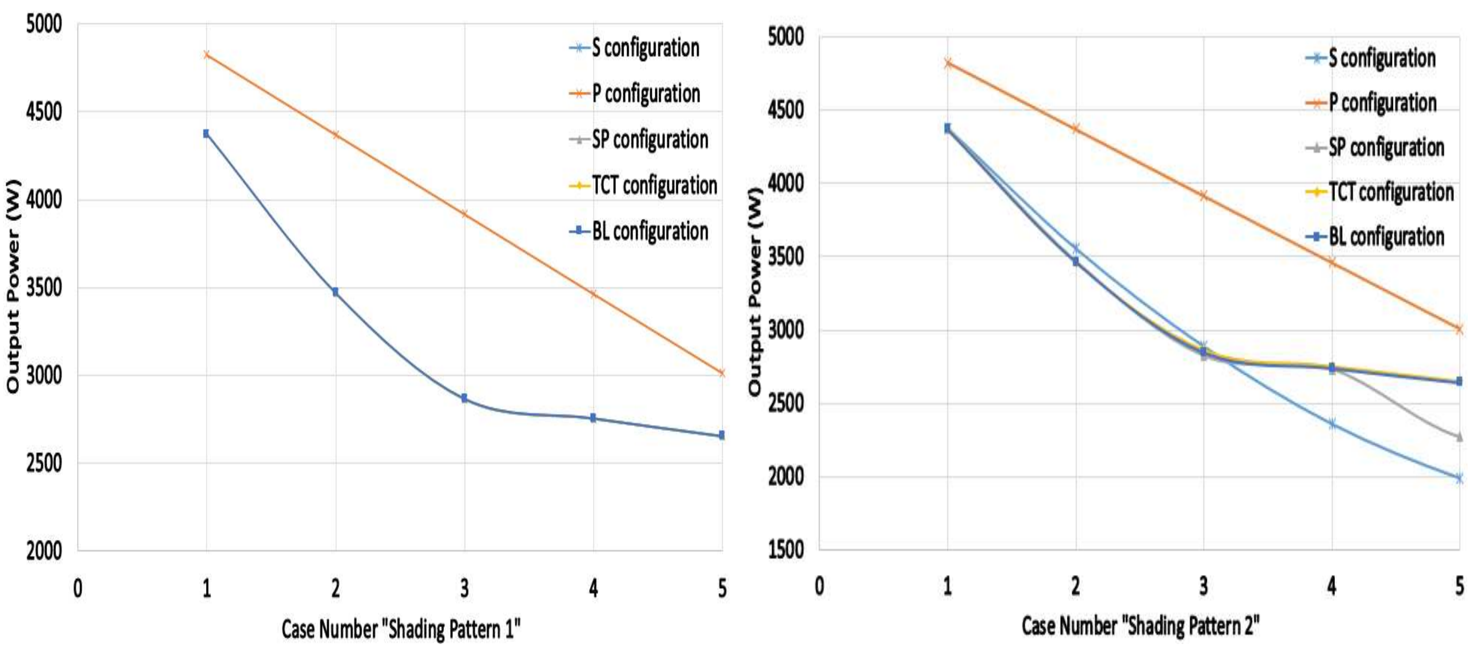

(a) (b)

Fig. 8. Partial Shading Patterns for Scenario 1: Row Level. (a) Output Power for Pattern 1, (b) Output power for Pattern 2

Table 6
Estimated R_s for the Multiple Array Configurations, Scenario 1: Row Level, Pattern 1

Case #	Estimated R_s (Ω) for Shading Pattern 1				
	S	P	SP	TCT	BL
Case 1	13.33689	0.022147	0.826446	0.826446	0.826446
Case 2	14.47387	0.023601	0.897666	0.897666	0.897666
Case 3	15.61524	0.025198	0.966184	0.966184	0.966184
Case 4	16.7392	0.027174	1.037344	1.037344	1.037344
Case 5	17.87949	0.029661	1.105705	1.105705	1.105705

Table 7
Estimated R_s for the Multiple Array Configurations, Scenario 1: Row Level, Pattern 2

Case #	Estimated R_s (Ω) for Shading Pattern 2				
	S	P	SP	TCT	BL
Case 1	14.05877	0.022279	0.848896	0.827267	0.835422
Case 2	15.9261	0.023609	0.921404	0.898473	0.906618
Case 3	17.75884	0.025253	0.990099	0.968992	0.975039
Case 4	19.604	0.027216	1.053297	1.037775	1.045369
Case 5	21.42704	0.029775	1.136493	1.109385	1.117318

Table 7 shows the estimated R_s for partial shading pattern 2. The S configuration has an increase by 1.8 Ω in the R_s. Moreover, the parallel configuration has the lowest rate of change in the R_s which is approximate equal to 0.002. SP, TCT and BL configurations has an increase of 0.07 Ω in the R_s among all testes cases in the row level partial shading conditions.

The FF indicator was also calculated for each examined partial shading patterns. Fig. 9(a) and Fig 9(b) illustrates the FF variations among the tested GCPV systems for shading pattern 1 and shading pattern 2 respectively. The P configuration shows that the FF has a value close to 73% among all tested case scenarios. However, a reduction in the FF was obtained across all other PV array configurations.

The Thermal voltage V_{te} across each PV array configuration during the tested partial shading pattern1 and pattern 2 are shown in Fig. 9(c) and Fig. 9(d) respectively. The threshold values of the V_{te} is taken from Table 4. It is evident that the V_{te} for P configuration is approximate equal to 1.44V which is exactly the same as the P configuration V_{te} threshold.

S, SP, TCT and BL configurations show that the value of V_{te} is lower than the value of V_{te} threshold in low partial shading conditions if: reduction in irradiance < 6000 W/m^2. However, in most partial shading conditions examined in this section, the obtained value of the V_{te} is greater than the value of V_{te} threshold if: reduction in the irradiance ≥ 6000 W/m^2.

From this section, the obtained results could be illustrated as the following:

- R_s could be a good indicator to predict/estimate partial shading conditions for S, SP, TCT and BL configurations. However, R_s cannot be used with P configuration since it does not change significantly during the increase/decrease of the partial shading conditions applied PV system.
- FF has a significant drop in its value while increasing the partial shading in the S, SP, TCT and BL configurations. This is not a proper indicator to be used with P configuration since it does not change among all tested partial shading conditions.
- When the reduction in the irradiance is greater or equal to 6000 W/m^2, the value of the V_{te} in most partial shading conditions is greater than the value of V_{te} threshold for S, SP, TCT and BL configurations. However, P configurations shows that the value of the V_{te} is almost equal to the value of V_{te} threshold.

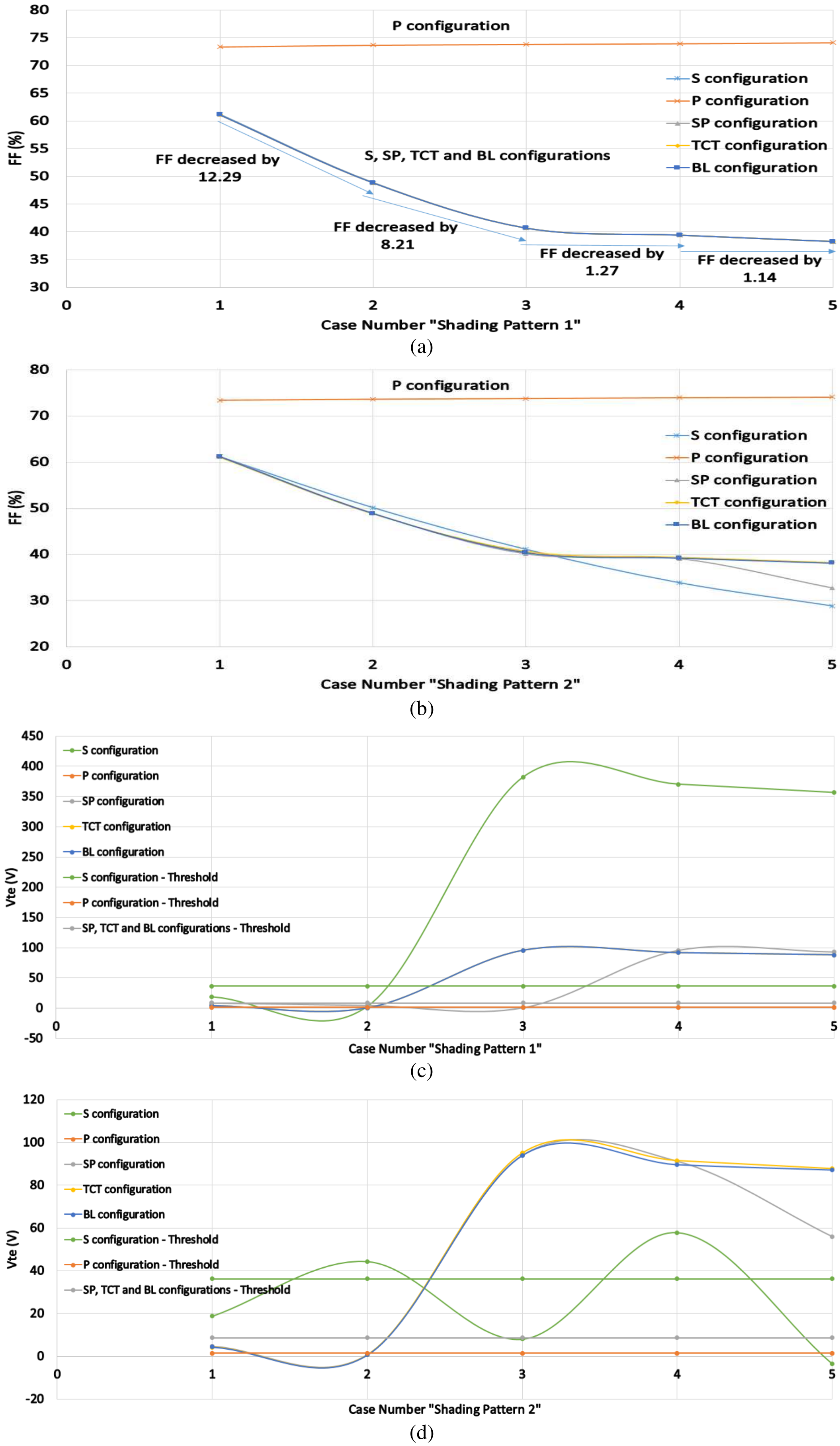

Fig. 9. FF and V_{te} Variations for Scenario 1: Row Level. (a) Fill Factor Variations for Pattern 1, (b) Fill Factor Variations for Pattern 2, (c) V_{te} Variations for Pattern 1, (d) V_{te} Variations for Pattern 2

4.3.2 Scenario 2: column level

This section is created to check the variations of the R_s, V_{te}, FF indicators when a partial shading conditions occurred in the PV array configuration on a column level (column of PV modules).

Fig. 10 shows two different partial shading patterns examined. The first partial shading pattern is applied on a column of PV modules at irradiance level equal to 500 W/m^2. However, the second shading pattern consists of various irradiance levels (100, 200, 500, 600, 800 and 900 W/m^2) applied to six PV modules.

Fig. 11(a) shows the maximum output power obtained in each PV array configuration under shading pattern 1. P, SP, TCT and BL configurations shows approximately the same maximum output power. Furthermore, S configuration provides the minimum output power during all examined case scenarios used in shading pattern 1. On the other hand, the maximum output power obtained from shading pattern 2 is illustrated in Fig. 11(b). The maximum output power could be evaluated at the P configuration. However, S configuration remains the worst configuration.

In each shading pattern (pattern 1 and 2), the series resistance (R_s) was estimated. Table 8 shows the estimated R_s for each PV array configuration for shading pattern 1. As can be noticed, Rs estimated for the S configuration is increasing by approximate to 1.68 **Ω**. This result can be calculated using the difference between case1 and case2, where the values of R_s are taken from the measured data explained in table 2:

$$Estimated\ R_s = Number\ of\ PV\ modules_{(at\ partial\ shading\ condition)} \times R_{s\,(at\ partial\ shading\ condition)}$$

$$Case1: Estimated\ R_s = \left(6_{\left(at\ 500\frac{W}{m^2}\right)} \times 0.789787\right) + \left(18_{\left(at\ 1000\frac{W}{m^2}\right)} \times 0.48484\right) = 13.47\ \Omega$$

$$Case2: Estimated\ R_s = \left(12_{\left(at\ 500\frac{W}{m^2}\right)} \times 0.789787\right) + \left(12_{\left(at\ 1000\frac{W}{m^2}\right)} \times 0.48484\right) = 15.30\ \Omega$$

$$Differance = Case2 - Case1 = 15.3 - 13.47 = 1.83\ \Omega \approx 1.68\ \Omega \text{ Obtianed by the I} - \text{V cuve}$$

Partial Shading Pattern 1

500 W/m^2	1000 W/m^2	1000 W/m^2	1000 W/m^2
500 W/m^2	1000 W/m^2	1000 W/m^2	1000 W/m^2
500 W/m^2	1000 W/m^2	1000 W/m^2	1000 W/m^2
500 W/m^2	1000 W/m^2	1000 W/m^2	1000 W/m^2
500 W/m^2	1000 W/m^2	1000 W/m^2	1000 W/m^2
500 W/m^2	1000 W/m^2	1000 W/m^2	1000 W/m^2

Case 1: First Column 500W/m^2

Case 2: First and Second Columns 500W/m^2

Case 3: First, Second and Third Columns 500W/m^2

Case4: First, Second, Third and Fourth Columns 500W/m^2

Partial Shading Pattern 2

100 W/m^2	1000 W/m^2	1000 W/m^2	1000 W/m^2
200 W/m^2	1000 W/m^2	1000 W/m^2	1000 W/m^2
500 W/m^2	1000 W/m^2	1000 W/m^2	1000 W/m^2
600 W/m^2	1000 W/m^2	1000 W/m^2	1000 W/m^2
800 W/m^2	1000 W/m^2	1000 W/m^2	1000 W/m^2
900 W/m^2	1000 W/m^2	1000 W/m^2	1000 W/m^2

Case 1: First Column unevenly shaded (pattern 2)

Case 2: First and Second Columns unevenly shaded (pattern 2)

Case 3: First, Second and Third Columns unevenly shaded (pattern 2)

Case 4: First, Second, Third and Fourth Columns unevenly shaded (pattern 2)

Fig. 10. Partial Shading Patterns for Scenario 2: Column Level

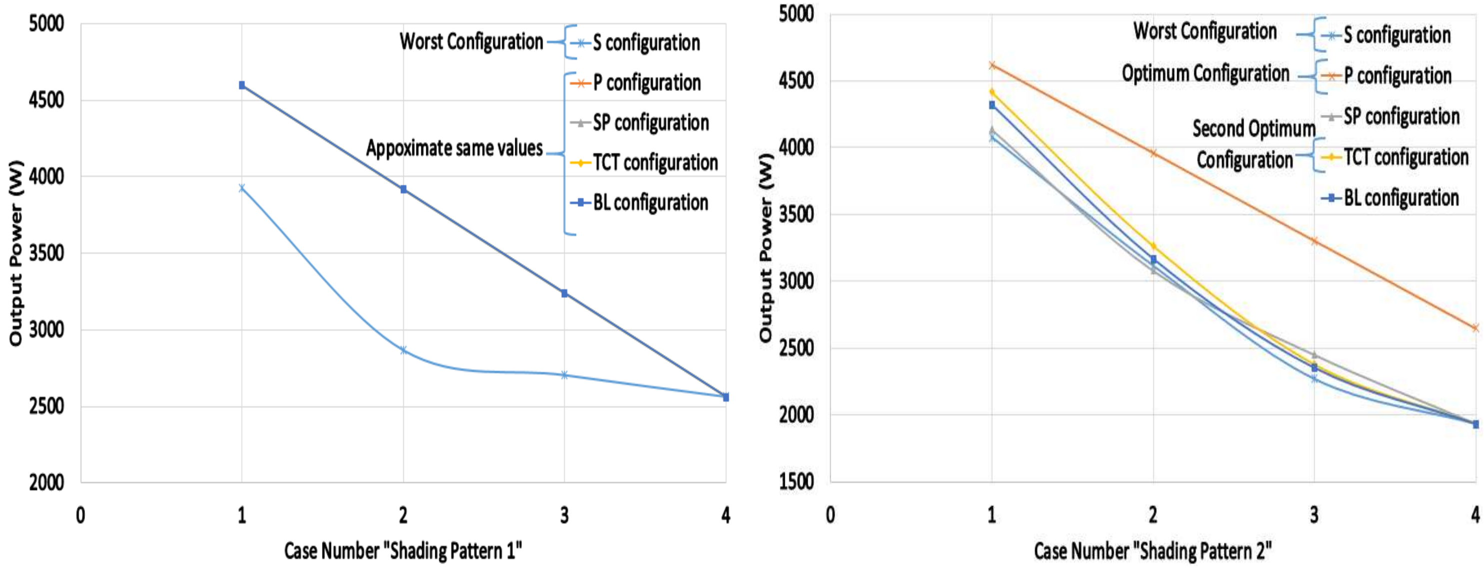

(a) (b)

Fig. 11. Partial Shading Patterns for Scenario 2: Column Level. (a) Output Power for Pattern 1, (b) Output power for Pattern 2

Additionally, the estimated series resistance for SP, TCT and BL configurations is increasing by approximate to 0.12 Ω. However, the parallel configuration remains at nearly constant series resistance between 0.02 – 0.03 Ω.

For the second shading pattern (non-uniform irradiance) the estimated R_s for SP, TCT and BL configurations is increasing by 0.3 Ω. The parallel configuration remains at the same R_s which is between 0.02 – 0.03 Ω. Similarly, the estimated series resistance for S configuration is increasing by 4.4 Ω while increasing the applied partial shading on the PV array configuration, this can be seen in Table 9 and described by the following mathematical calculations, where the values of R_s are taken from the measured data explained in table 2:

$$Measured\ R_s = Number\ of\ PV\ modules_{(at\ partail\ shading\ condition)} \times R_{s\ (at\ partial\ shading\ condition)}$$

$$Case1: Measured\ R_s$$

$$= \left(1_{\left(at\ 100\frac{W}{m^2}\right)} \times 3.241\right) + \left(1_{\left(at\ 200\frac{W}{m^2}\right)} \times 1.688\right) + \left(1_{\left(at\ 500\frac{W}{m^2}\right)} \times 0.789787\right)$$
$$+ \left(1_{\left(at\ 600\frac{W}{m^2}\right)} \times 0.6988\right) + \left(1_{\left(at\ 800\frac{W}{m^2}\right)} \times 0.5677\right) + \left(1_{\left(at\ 900\frac{W}{m^2}\right)} \times 0.5378\right)$$
$$+ \left(18_{\left(at\ 1000\frac{W}{m^2}\right)} \times 0.48484\right) = 16.25\ \Omega$$

$$Case2: Measured\ R_s$$

$$= \left(2_{\left(at\ 100\frac{W}{m^2}\right)} \times 3.241\right) + \left(2_{\left(at\ 200\frac{W}{m^2}\right)} \times 1.688\right) + \left(2_{\left(at\ 500\frac{W}{m^2}\right)} \times 0.789787\right)$$
$$+ \left(2_{\left(at\ 600\frac{W}{m^2}\right)} \times 0.6988\right) + \left(2_{\left(at\ 800\frac{W}{m^2}\right)} \times 0.5677\right) + \left(2_{\left(at\ 900\frac{W}{m^2}\right)} \times 0.5378\right)$$
$$+ \left(12_{\left(at\ 1000\frac{W}{m^2}\right)} \times 0.48484\right) = 20.865\ \Omega$$

$$Differance = Case2 - Case1 = 20.865 - 16.25 = 4.6\ \Omega \approx 4.4\ \Omega \text{ Obtianed by the I} - \text{V cuve}$$

Table 8

Estimated R_s for the Multiple Array Configurations, Scenario 2: Column Level, Pattern 1

Case #	Estimated R_s (Ω) for Shading Pattern 1				
	S	P	SP	TCT	BL
Case 1	13.8754	0.022921	0.818197	0.818197	0.818197
Case 2	15.55936	0.025198	0.898957	0.898957	0.898957
Case 3	17.26519	0.028329	1.012146	1.012146	1.012146
Case 4	18.93581	0.033034	1.176471	1.176471	1.176471

Table 9
Estimated R_s for the Multiple Array Configurations, Scenario 2: Column Level, Pattern 2

Case #	Estimated R_s (Ω) for Shading Pattern 2				
	S	P	SP	TCT	BL
Case 1	16.85772	0.022861	0.83675	0.819403	0.823045
Case 2	21.33106	0.025054	0.961538	0.918274	0.929195
Case 3	25.75992	0.02809	1.186662	1.106195	1.119821
Case 4	30.08424	0.032468	1.845018	1.845359	1.845359

Fig. 12(a) and Fig. 12(b) illustrates the FF variations among the tested PV array configuration systems for shading pattern 1 and shading pattern 2 respectively. Shading pattern 1 shows that P, SP, TCT and BL configurations have a value of FF approximate to 74% among all tested cases. However, a reduction in the FF was only obtained across the S configuration. Shading pattern 2 (non-uniform shading) shows a different results comparing to shading pattern 1 (uniform shading), these results could be illustrated as the following:

- The estimated FF for the P configuration under non-uniform and uniform shading patterns are exactly equal.
- There is a huge reduction in the FF for S, SP, TCT and BL configurations in the non-uniform shading pattern conditions.
- Fig. 12(a) shows that the value of the FF for the S configuration at case 4 is equal to 74% because in this particular shading case, the percentage of shading among all PV modules are equal.

The Thermal voltage V_{te} across each PV array configuration during the tested partial shading pattern1 and pattern 2 are shown in Fig. 12(c) and Fig. 9(d) respectively. The threshold values of the V_{te} is taken from Table 4. It is evident that the V_{te} for P configuration is approximate equal to 1.44V which is exactly the same as the P configuration V_{te} threshold. The estimated values of the V_{te} for SP, TCT and BL configurations are exactly the same as the V_{te} threshold during shading pattern 1. However, the estimated V_{te} for S configuration is greater than the value of the V_{te} threshold if: Reduction in irradiance $\geq$ 6000 W/m^2.

Fig. 12(d) shows that the estimated V_{te} is exactly the same as the V_{te} threshold for shading pattern 2. SP, TCT and BL configurations proves that when the reduction in the irradiance is greater than 2900 W/m^2 the estimated value of V_{te} is always greater than V_{te} threshold. Moreover, S configuration shows that the value of the V_{te} is greater than V_{te} threshold if: Reduction in irradiance $\geq$ 6000 W/m^2.

In conclusion, this section shows some results on the performance of the examined PV array configurations under uniform and non-uniform partial shading patterns. The main findings could be illustrated as the following:

- Under uniform shading patterns which effects on a column of PV modules, the output power for P, SP, TCT and BL configurations are exactly the same. Furthermore, the S configuration shows the least output power among all PV array configurations.
- Under non-uniform shading patterns which effects on a column of PV modules, the optimum output power was estimated for the parallel configuration.
- The series resistance R_s is a good indicator for detecting/predicting partial shading conditions for S, SP, TCT and BL configurations since the value of the R_s change significantly while increasing the partial shading conditions applied to the PV configurations.
- The Fill factor (FF) indicator could be used with SP, TCT and BL configurations only under non-uniform irradiance conditions. Furthermore, there is a large drop in the value of FF for the S configuration under uniform and non-uniform irradiance levels.
- The value of the V_{te} could be used as a proper indicator for detecting partial shading conditions for S, SP, TCT and BL configuration under non-uniform partial shading conditions affecting the GCPV plants.

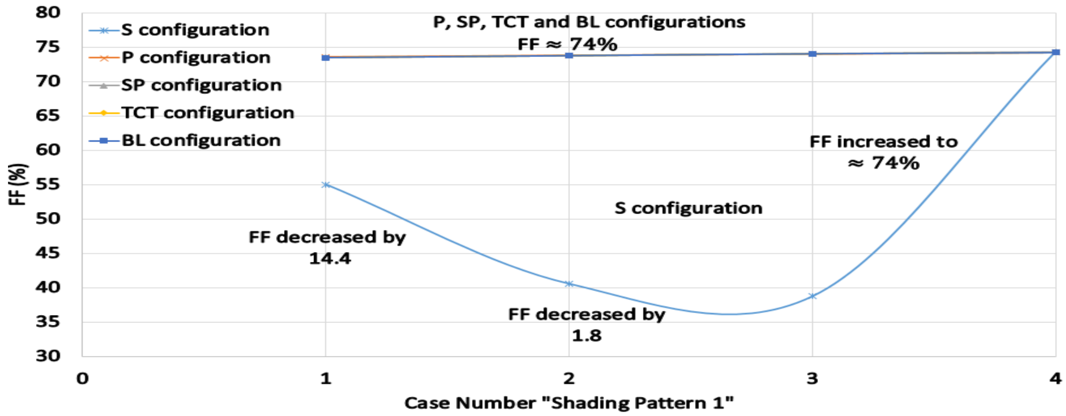

(a)

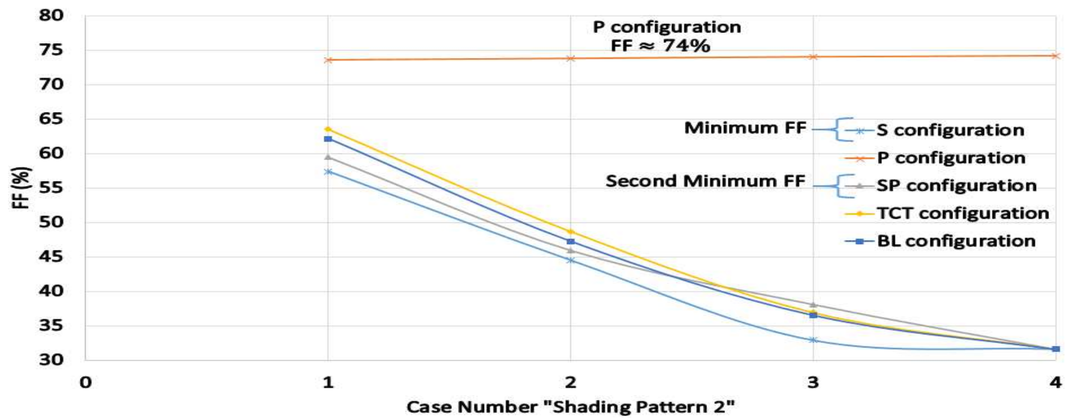

(b)

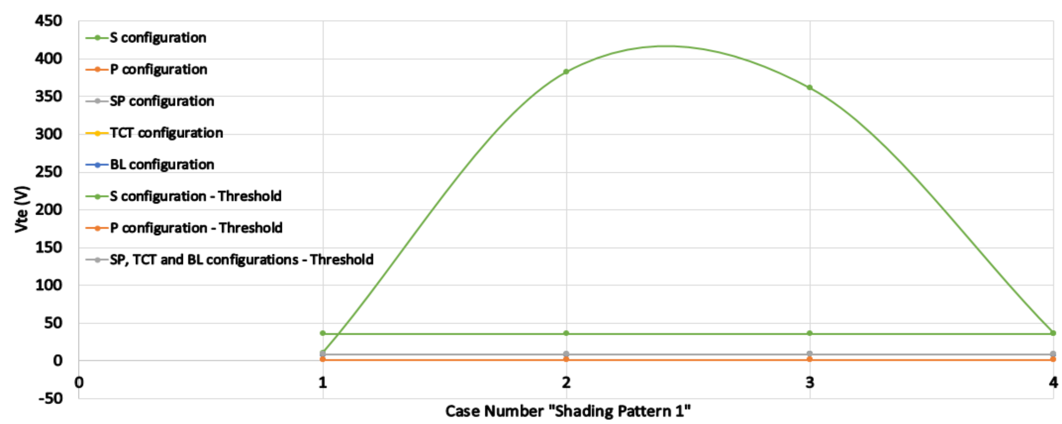

(c)

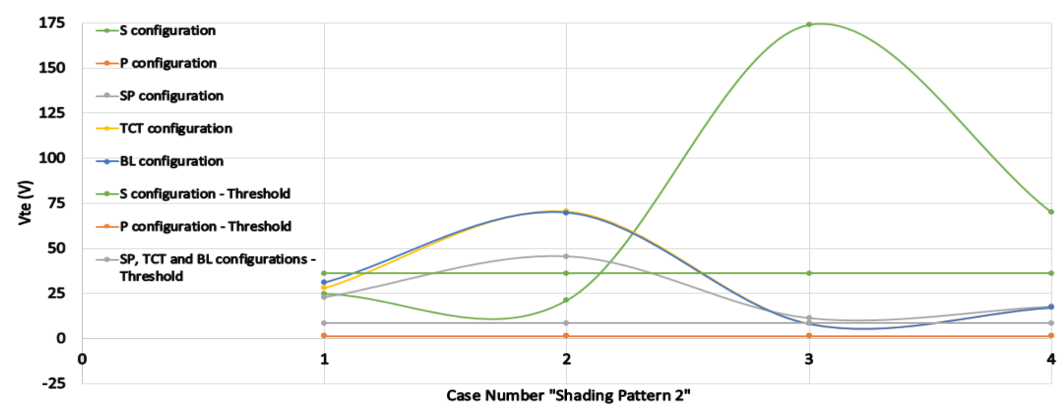

(d)

Fig. 12. FF and V_{te} Variations for Scenario 2: Column Level. (a) Fill Factor Variations for Pattern 1, (b) Fill Factor Variations for Pattern 2, (c) V_{te} Variations for Pattern 1, (d) V_{te} Variations for Pattern 2

4.3.3 Scenario 3: faulty PV modules

This section is created to check the variations of the R_s, V_{te}, FF indicators when a faulty PV modules have been a raised in the PV array configurations.

Two faulty scenarios were carried out to estimate the output performance for each PV array configuration under faulty PV modules. Fig. 13 illustrates both cases which can be described by the following:

1. Row level: six different scenarios were tested to estimate the faulty PV modules which are disconnected (short circuit the PV module) from a row of the PV array configuration.
2. Column level: four different scenarios were tested to estimate the faulty PV modules which are disconnected from the entire column of the PV array configuration.

The PV modules irradiance and temperature level are at standard test conditions: 1000W/m^2 and 25 ^{o}C respectively.

Fig. 14(a) and Fig 14(b) shows that the configurations S and P provides the highest maximum output power among all PV array configurations. The second maximum output power is achieved by the SP configuration. However, the minimum output power is estimated for the TCT configuration among all faulty PV case scenarios.

The estimated series resistance R_s for the row-level PV faulty conditions are illustrated in Table 10. The S configuration shows that R_s is decreasing by 0.49 Ω while disconnecting one PV module. This result is approximate equal to the measured value of R_s among one PV module (0.48484 Ω) under STC as shown previously in Table 5.

The estimated R_s for the P configuration among all faulty scenarios is approximately equal to 0.02 Ω. The value of R_s when a PV string is disconnected from the PV array configuration is equal to 1.007 Ω for SP, TCT and BL configurations, this value cloud be calculated using (16) as the following:

$$Estimated\ R_s for\ one\ PV\ module = \frac{R_{s\ (Obtained\ from\ the\ I-V\ Curve)} \times 3\ _{(number\ of\ PV\ columns)}}{6\ _{(number\ of\ PV\ modules\ in\ one\ PV\ row\ "PV\ String")}}$$

$$0.48484 = \frac{R_{s\ (Obtained\ from\ the\ I-V\ Curve)} \times 3\ (Since\ one\ PV\ string\ is\ completly\ disconnected)}{6}$$

$$R_{s\ (Obtained\ from\ the\ I-V\ Curve)} = 0.97\ \Omega \approx 1.007\ \Omega$$

The estimated series resistance R_s for the column-level PV faulty conditions are illustrated in Table 11. As can be noticed that the value of R_s in the S and SP configurations is decreased while increasing the number of faulty PV modules. The estimated R_s for TCT and BL is increasing for the first three PV faulty conditions. However, the estimated R_s is equal to 0.63 Ω when disconnecting an entire PV column form the SP, TCT and BL array configurations. This result could be estimated using (16) as the following:

$$Estimated\ R_s for\ one\ PV\ module = \frac{R_{s\ (Obtained\ from\ the\ I-V\ Curve)} \times 4\ _{(number\ of\ PV\ columns)}}{5\ _{(number\ of\ PV\ modules\ in\ one\ PV\ row\ "PV\ String")}}$$

$$0.48484 = \frac{R_{s\ (Obtained\ from\ the\ I-V\ Curve)} \times 4\ (Since\ one\ PV\ string\ is\ completly\ disconnected)}{5}$$

$$R_{s\ (Obtained\ from\ the\ I-V\ Curve)} = 0.61\ \Omega \approx 0.63\ \Omega$$

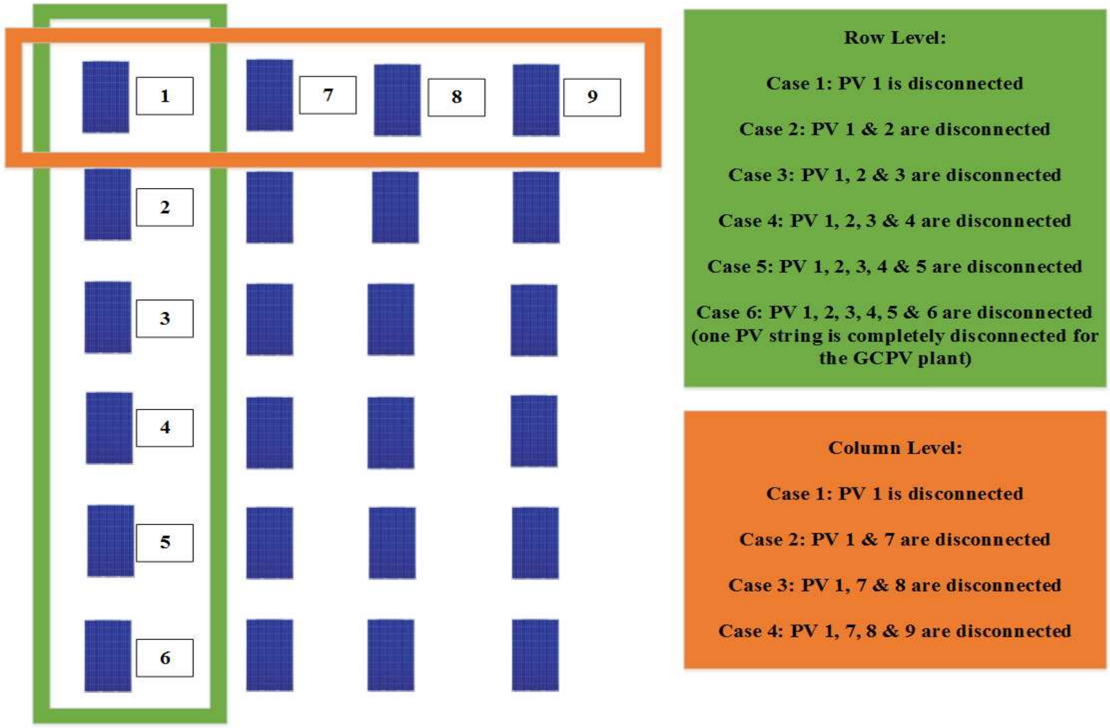

Fig. 13. PV Faulty Conditions for Scenario 3: Faulty PV Modules

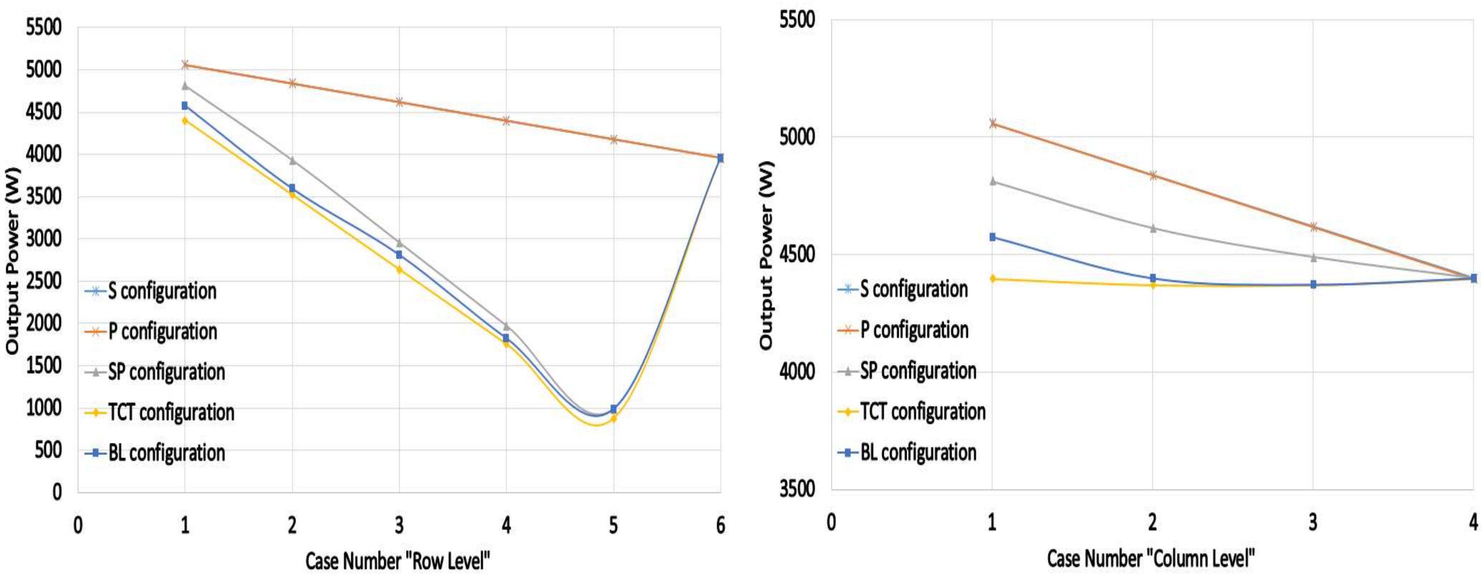

(a) (b)

Fig. 14. Output Power for Scenario 3: Faulty PV Modules. (a) Output Power for Pattern 1, (b) Output power for Pattern 2

Fig. 15(a) and Fig. 15(b) illustrates the FF variations among the tested PV array configurations using faulty conditions: row-level and column level respectively. Row-level PV faulty conditions show that S, P and TCT configurations have a value of FF approximate to 73.2% among all tested scenarios. However, a reduction in the FF was only obtained across the SP and BL configurations.

The column-level PV faulty conditions shows that the FF for the S and P configuration remains at 73.2%. Furthermore, there is a huge reduction in the estimated FF for both TCT and BL configurations. The only configuration which has an increase in the estimated values of the FF was obtained for the SP configuration.

As shown in Fig. 15(a) at case 6 (Faulty PV string) the estimated value of the FF across all PV array configurations is equal to 73.2%. Similar results obtained for case4 (faulty column) illustrated in Fig 15(b).

The Thermal voltage V_{te} estimated for each PV array configuration under faulty PV modules conditions (row-level and column-level) are shown in Fig. 15(c) and Fig. 9(d) respectively. From Fig. 15(c), it is evident that V_{te} for P configuration is equal to 1.36V among all PV faulty conditions, this result is approximately equal to P configuration V_{te} threshold: 1.44V. The estimated value of the V_{te} for S, SP, TCT and BL configurations is decreased while increasing the number of faulty PV modules in the PV array configuration due to the decrease in the V_{mp}. Despite the decrease of V_{oc}, the value of V_{mp} is multiplied by a factor of 2, therefore, V_{te} is also decreasing. This results can be expressed by the following:

$$V_{te} \downarrow = \frac{(2V_{mp} \downarrow\downarrow - V_{oc} \downarrow)(I_{sc} - I_{mp})}{I_{mp} - (I_{sc} - I_{mp}) \ln(\frac{I_{sc} - I_{mp}}{I_{sc}})}$$

Different results obtained at case6 in Fig. 15(c), where a faulty PV string occurred in each PV configuration. The value of V_{te} for the SP, TCT and BL is increased because the value of the I_{sc} and $_{Imp}$ is decreased:

$$V_{te} \uparrow = \frac{(2V_{mp} \downarrow\downarrow - V_{oc} \downarrow)(I_{sc}\downarrow - I_{mp}\downarrow)}{I_{mp}\downarrow - (I_{sc}\downarrow - I_{mp}\downarrow) \ln\left(\frac{I_{sc}\downarrow - I_{mp}\downarrow}{I_{sc}\downarrow}\right)} \quad \textit{denominator is decreasing more than numerator}$$

Similar results obtained for the estimated V_{te} in the column-level faulty PV conditions as shown in Fig 15(d). The main findings of this section can be listed as the following:

- When the number of faulty PV modules in increasing the estimated R_s is decreasing in S, SP TCT and BL configurations.
- The FF for the S and P configurations among all faulty PV conditions remains at 73.2%.
- The estimated value of V_{te} for S, SP, TCT and BL configurations is decreased while increasing the number of faulty PV modules. However, in case of the faulty PV string occurred in the PV system, the value of the V_{te} is increased only in SP, TCT and BL configurations.
- P configuration has approximately constant levels of FF and V_{te} among all tested PV faulty conditions.

Table 10

Estimated R_s for the Multiple Array Configurations, Scenario 3: PV Faulty Conditions, Row Level

Case #	Estimated R_s (Ω)				
	S	P	SP	TCT	BL
Case 1	11.57273	0.022096	0.800641	0.631313	0.829876
Case 2	11.08033	0.023095	1.01688	0.505306	0.591541
Case 3	10.58574	0.024196	0.889442	0.379219	0.596659
Case 4	10.08065	0.025408	0.596659	0.253936	0.333778
Case 5	9.581603	0.026748	0.299043	0.128304	0.298151
Case 6	9.077156	0.028226	1.00776	1.00776	1.00776

Table 11

Estimated R_s for the Multiple Array Configurations, Scenario 3: PV Faulty Conditions, Column Level

Case #	Estimated R_s (Ω)				
	S	P	SP	TCT	BL
Case 1	11.57273	0.022096	0.800641	0.631313	0.829876
Case 2	11.08033	0.023095	0.764526	0.884173	0.913242
Case 3	10.58574	0.024196	0.693481	1.135203	1.135203
Case 4	10.08065	0.025408	0.631313	0.631313	0.631313

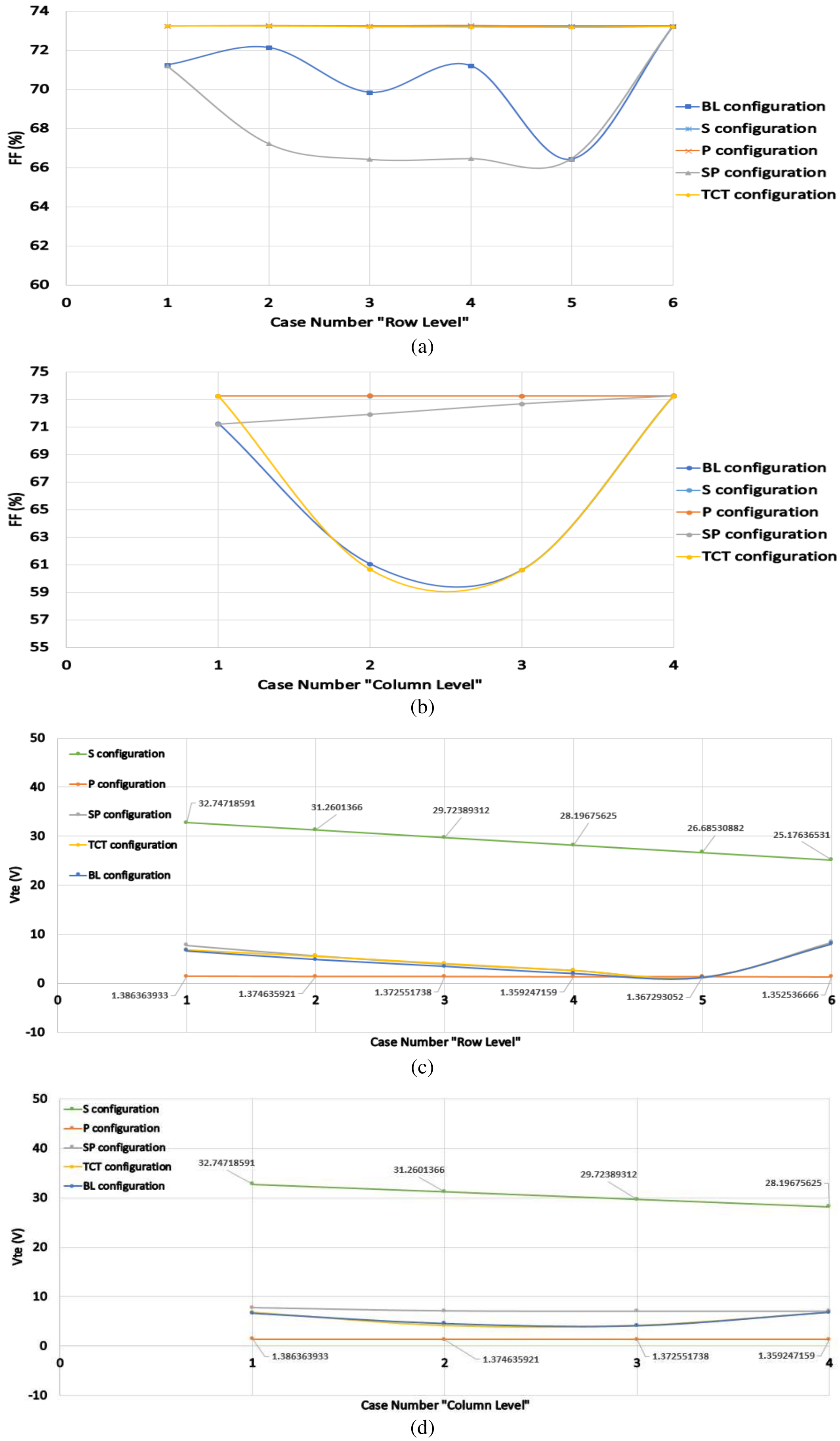

Fig. 15. FF and V_{te} Variations for Scenario 3: Faulty PV Conditions. (a) Fill Factor Variations for Row Level PV Faulty Conditions, (b) Fill Factor Variations for Column Level PV Faulty Conditions, (c) V_{te} Variations for Row Level PV Faulty Conditions, (d) V_{te} Variations for Column Level PV Faulty Conditions

5. *Discussion*

In this paper a brief modelling, simulation and data analysis of various partial shading and PV faulty modules conditions have been discussed. Multiple diagnostic indicators have been used to compare the performance of each PV array configuration such as short circuit current (I_{sc}), current at maximum power point (I_{mpp}), open circuit voltage (V_{oc}), voltage at maximum power point (V_{mpp}), series resistance (R_s), fill factor (FF) and thermal voltage (V_{te}). Few of these indictors have been demonstrated by F. Belhachat [6].

However, the partial shading conditions applied in this paper is not static as shown in [6, 7, 9 and 13], which means that the partial shading conditions are either increasing or decreasing among all PV modules. Additionally, in order to test the performance of each PV array configuration under faulty PV conditions, from 1 to 6 Faulty PV modules have been disconnected in order to compare between each PV indicator variations, this scenario has been demonstrated in section 4.3.3. Currently, there are few research articles which combines between faulty PV conditions with multiple PV array configurations. Therefore, this section is one of the major contribution for this paper.

The obtained results of this research can be divided into four main categories:

1. PV array configurations under standard test condition (STC):
    - The S, P, SP, TCT and BL configurations provide the same maximum output power.
    - FF for all PV array configurations is approximately equal to 73.2%.
    - New mathematical expressions have been derived for estimating the value of the series resistance R_s across one PV module in all tested PV array configurations.

2. PV array configurations under uniform partial shading conditions:
    - P configuration provides the maximum output power when one to five rows or/and one to four columns are completely shaded.
    - S, SP, TCT and BL configurations have an increase of the R_s while increase the uniform shading across the PV modules. While P configuration series resistance remains at the same value which is approximate to 0.02 Ω.
    - FF for the S, SP, TCT and BL configurations have a significant drop in its value while increasing the uniform partials shading condition applied to a row of PV modules. However, the P configuration FF remains at a threshold of 74%.
    - The value of V_{te} is not a proper indicator for predicting/estimating the change in the partial shading conditions for S, SP, TCT and BL since it does not change among all tested uniform partial shading conditions.

3. PV array configurations under non-uniform partial shading conditions:
    - P configuration provides the maximum output power when one to five rows and/or one to four columns are completely shaded. Furthermore, TCT configuration provided the second optimum output power among all other PV array configurations.
    - S, SP, TCT and BL configurations have an increase of the R_s while increase the non-uniform shading across the PV modules. While P configuration series resistance remains at the same value which is approximate to 0.02 Ω.
    - SP, TCT and BL configurations proves that when the reduction in the irradiance is greater than 2900 W/m^2 the estimated value of V_{te} is always greater than V_{te} threshold. Moreover, S configuration shows that the value of the V_{te} is greater than V_{te} threshold if: Reduction in irradiance $\geq$ 6000 W/m^2.

4. <u>PV array configurations under faulty PV conditions:</u>
   - P configuration provides the maximum output power when one to five PV modules are faulty in a row of PV modules and when one to four PV modules are disconnected from a column of PV modules in the PV array configuration.
   - The estimation of the R_s of a single PV module in the PV array configurations can be calculated using the following mathematical expression:

S configuration

$$\frac{R_{s\,(Obtained\ from\ the\ I-V\ Curve)}}{24_{(total\ PV\ module\ in\ the\ PV\ array\ configuration)}}$$

P configuration

$$R_{s\,(Obtained\ from\ the\ I-V\ Curve)} \times 24_{(total\ PV\ module\ in\ the\ PV\ array\ configuration)}$$

SP, TCT and BL configurations

$$\frac{R_{s\,(Obtained\ from\ the\ I-V\ Curve)} \times 4_{\,(number\ of\ PV\ columns)}}{6_{\,(number\ of\ PV\ modules\ in\ one\ PV\ row\ "PV\ String")}}$$

   - The estimated value of V_{te} for S, SP, TCT and BL configurations is decreased while increasing the number of faulty PV modules. However, in case of faulty PV string occurred in the PV system, the value of the V_{te} is increased only in SP, TCT and BL configurations.
   - The FF for the S and P configurations among all faulty PV conditions remains at 73.2%. However, for all other PV configurations the estimated value of the FF is either increasing or decreasing.

From the obtained results, it is evident that the variations of I_{sc}, I_{mpp}, V_{oc}, and V_{mpp} are not shown. This is because the value of these indicators have been widely discussed by many research articles such as [6, 7, 9 and 13]. However, all listed references does not include the increase or decrease of shading patterns among all PV configurations, additionally, there are few of discussions about faulty PV modules in multiple PV array configurations.

Table 12, 13 and 14 illustrates the variations for all indicators used in this article among all examined partial shading and faulty PV conditions in the S, P, SP, TCT and BL PV array configurations. Three different symbols are used to show whether the value of the indicator has an "↓" decrease, "↑" increase, "–" no change in its value and ↓↑ decrease or increase in the value of the indicator. A brief discussion of the indicators R_s, FF and V_{te} are is available in section 4.

The S, SP, TCT and BL configurations have always a reduction in the value of V_{oc} while increasing the uniform, non-uniform shading conditions and increasing the number of faulty PV modules. The P configuration has a reduction in the V_{oc} among all shading patterns, however, V_{oc} remains constant while increasing or decreasing the number of faulty PV modules.

In most tested conditions, the value of the I_{sc} has no change for the S, SP, TCT and BL configurations. The P configuration proves that the value of I_{sc} is always decreasing while increasing the uniform, non-uniform shading conditions and increasing the number of faulty PV modules.

The voltage at maximum power point (V_{mpp}) is not a proper indicator for estimating/predicting partial shading conditions or/and faulty PV modules in the S, SP, TCT and BL configuration because in each tested condition the value of V_{mpp} is either increased or decreased. However, this comment is not applicable for the P configuration because the value of the V_{mpp} is always decreasing while increasing the partial shading conditions applied to the PV plant.

The last indicator, I_{mpp} is a proper indicator to estimate/predict partial shading conditions in all examined PV array configurations since the value of the indicator is decreasing while increasing shading conditions. The value of I_{mpp} does not change while increasing/decreasing number of faulty PV modules in S, SP, TCT and BL configurations. However, it does change significantly for the P configuration.

Table 12
Change in the Estimated Indicators on Each PV Array Configuration

Scenario	PV array configurations													
	S							P						
	I_{sc}	I_{mpp}	V_{oc}	V_{mpp}	R_s	FF	V_{te}	I_{sc}	I_{mpp}	V_{oc}	V_{mpp}	R_s	FF	V_{te}
Increasing uniform shading on PV row	-	↓	↓	↓↑	↑	↓	↓↑	↓	↓	↓	↓	-	-	-
Increasing non-uniform shading on PV row	-	↓	↓	↓↑	↑	↓	↓↑	↓	↓	↓	↓	-	-	-
Increasing uniform shading on PV column	-	↓	↓	↓↑	↑	↓↑	↓↑	↓	↓	↓	↓	-	-	-
Increasing non-uniform shading on PV column	-	↓	↓	↓↑	↑	↓	↓	↓	↓	↓	↓	-	-	-
Increasing faulty PV modules in PV row	-	-	↓	↓	↓	-	↓	↓	↓	-	-	↑	-	↓
Increasing faulty PV modules in PV column	-	-	↓	↓	↓	-	↓	↓	↓	-	-	↑	-	↓

Table 13
Change in the Estimated Indicators on Each PV Array Configuration

Scenario	PV array configurations													
	SP							TCT						
	I_{sc}	I_{mpp}	V_{oc}	V_{mpp}	R_s	FF	V_{te}	I_{sc}	I_{mpp}	V_{oc}	V_{mpp}	R_s	FF	V_{te}
Increasing uniform shading on PV row	-	↓	↓	↓↑	↑	↓↑	↑	-	↓	↓	↓↑	↑	↓	↓↑
Increasing non-uniform shading on PV row	-	↓	↓	↓↑	↑	↓	↓↑	-	↓	↓	↓↑	↑	↓	↓↑
Increasing uniform shading on PV column	-	↓	↓	↓	↑	-	-	↓	↓	↓	↓↑	↑	-	-
Increasing non-uniform shading on PV column	-	↓	↓	↓	↑	↓	↓↑	↓	↓	↓	↓↑	↑	↓	↓↑
Increasing faulty PV modules in PV row	-	-	↓	↓	↓↑	↓	↓	-	-	↓	↓	↓	-	↓
Increasing faulty PV modules in PV column	-	-	↓	↓	↓	↑	↓	-	-	↓	↓	↓	↓	↓

Table 14
Change in the Estimated Indicators on Each PV Array Configuration

Scenario	PV array configuration						
	BL						
	I_{sc}	I_{mpp}	V_{oc}	V_{mpp}	R_s	FF	V_{te}
Increasing uniform shading on PV row	-	↓	↓	↓↑	↑	↓	↓↑
Increasing non-uniform shading on PV row	-	↓	↓	↓↑	↑	↓	↓↑
Increasing uniform shading on PV column	↓	↓	↓	↓	↑	-	-
Increasing non-uniform shading on PV column	↓	↓	↓	↓↑	↑	↓	↓↑
Increasing faulty PV modules in PV row	-	-	↓	↓	↓	↓↑	↓
Increasing faulty PV modules in PV column	-	-	↓	↓	↓↑	↓	↓

6. *Conclusion*

In this paper, multiple PV array configurations including series (S), parallel (P), series-parallel (SP), total-cross-tied (TCT) and bridge-lined (BL) have been tested under various partial shading and faulty photovoltaic (PV) conditions. Several indicators such as short circuit current (I_{sc}), current at maximum power point (I_{mpp}), open circuit voltage (V_{oc}), voltage at maximum power point (V_{mpp}), series resistance (R_s), fill factor (FF) and thermal voltage (V_{te}) have been used to compare the obtained results from the partial shading and PV faulty conditions. MATLAB/Simulink software is used to perform the simulation and data analysis for each examined PV array configuration.

The variations for all indicators across all PV array configurations have been reported and compared briefly. Additionally, new mathematical expressions have been derived to estimate the value of the series resistance across a single PV module in each PV array configuration under standard test conditions (STC) and faulty PV modules.

Finally, this study gives a useful information on the main parameters that could be used for estimating/predicting partial shading conditions in all examined PV array configurations. Therefore, the results obtained from this study could be enhanced by creating a generic algorithm using machine learning techniques for detecting faulty PV modules in multiple PV array configurations or/and creating a reconfigurable PV array system to improve the power generation in grid-connected PV (GCPV) plants.

7. *Acknowledgment*

The authors would like to acknowledge the financial assistant to the University of Huddersfield, Engineering and Computing Department.

Appendix A. MATLAB/Simulink model for the examined PV array configurations.

Series (S) Configuration:

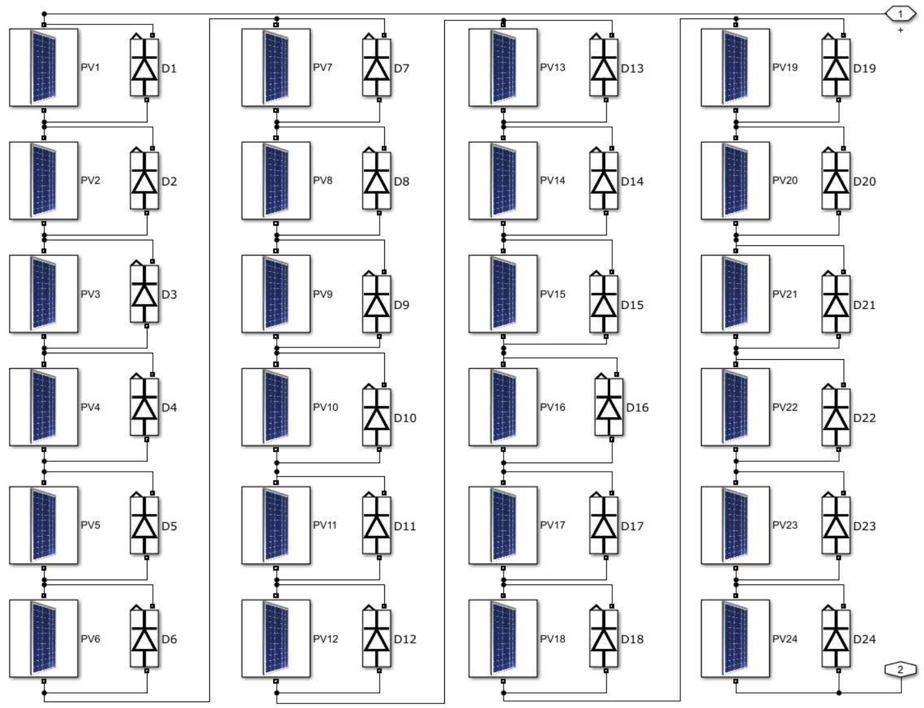

Parallel (P) Configuration:

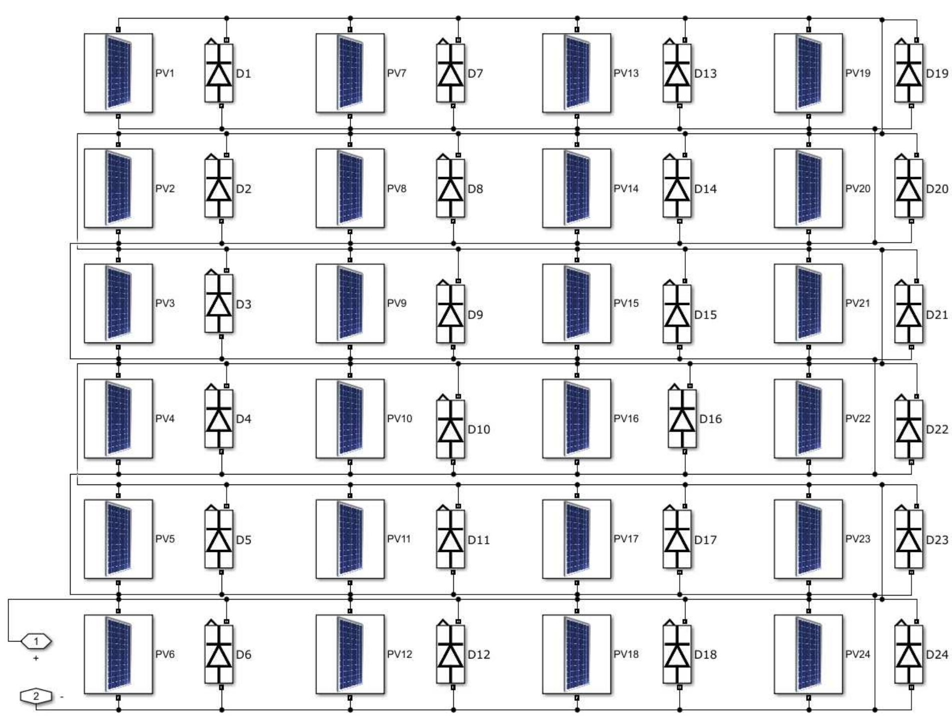

Series-Parallel (SP) Configuration:

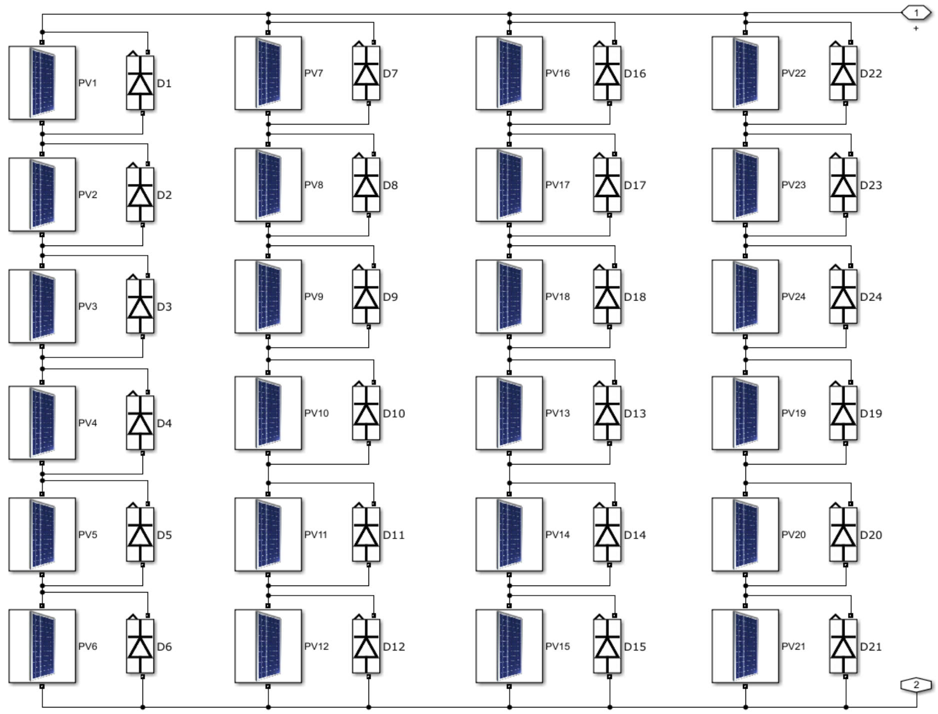

Total-Cross-Tied (TCT) Configuration:

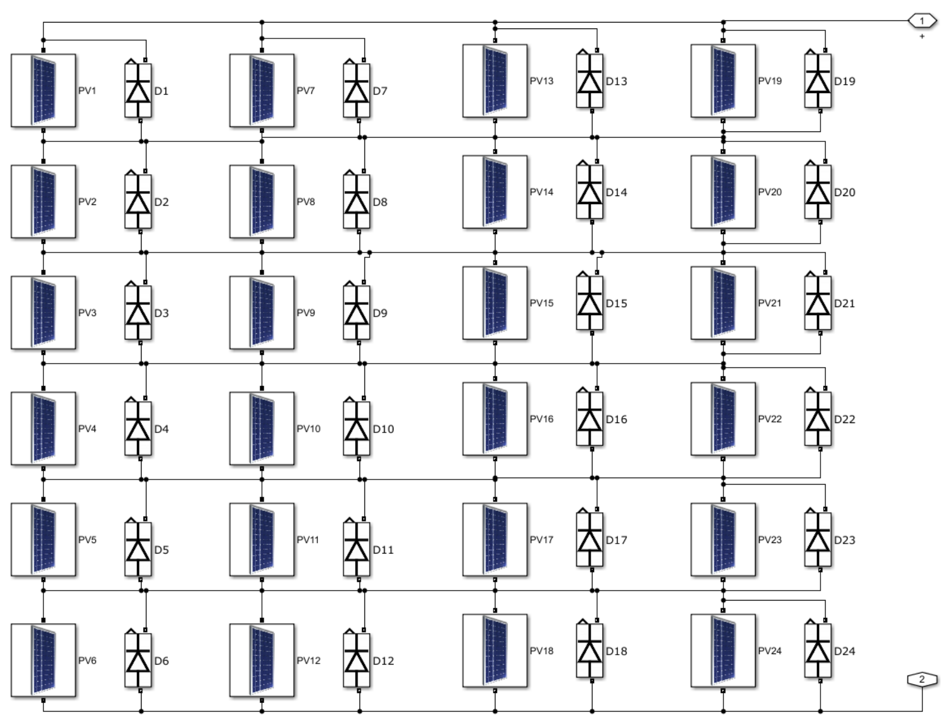

Bridge-Linked (BL) Configuration:

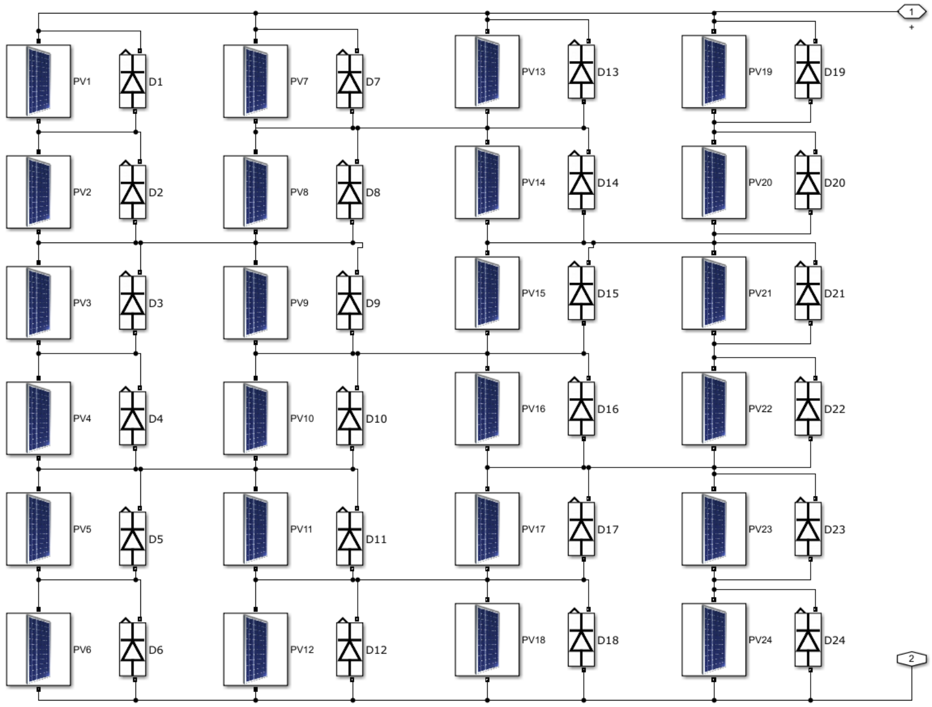

References

[1] Makrides, G., Zinsser, B., Schubert, M., & Georghiou, G. E. (2014). Performance loss rate of twelve photovoltaic technologies under field conditions using statistical techniques. *Solar Energy*, *103*, 28-42.

[2] Lappalainen, K., & Valkealahti, S. (2017). Output power variation of different PV array configurations during irradiance transitions caused by moving clouds. *Applied Energy*, *190*, 902-910.

[3] Bai, J., Cao, Y., Hao, Y., Zhang, Z., Liu, S., & Cao, F. (2015). Characteristic output of PV systems under partial shading or mismatch conditions. *Solar Energy*, *112*, 41-54.

[4] Di Vincenzo, M. C., & Infield, D. (2013). Detailed PV array model for non-uniform irradiance and its validation against experimental data. *Solar Energy*, *97*, 314-331.

[5] Yeung, R. S. C., Chung, H. S. H., Tse, N. C. F., & Chuang, S. T. H. (2017). A global MPPT algorithm for existing PV system mitigating suboptimal operating conditions. *Solar Energy*, *141*, 145-158.

[6] Belhachat, F., & Larbes, C. (2015). Modeling, analysis and comparison of solar photovoltaic array configurations under partial shading conditions. *Solar Energy*, *120*, 399-418.

[7] Mohammadnejad, S., Khalafi, A., & Ahmadi, S. M. (2016). Mathematical analysis of total-cross-tied photovoltaic array under partial shading condition and its comparison with other configurations. *Solar Energy*, *133*, 501-511.

[8] Wang, Y. J., & Hsu, P. C. (2011). An investigation on partial shading of PV modules with different connection configurations of PV cells. *Energy*, *36*(5), 3069-3078.

[9] Ramaprabha, R., & Mathur, B. L. (2012). A comprehensive review and analysis of solar photovoltaic array configurations under partial shaded conditions. *International Journal of Photoenergy*, *2012*.

[10] Ishaque, K., & Salam, Z. (2013). A review of maximum power point tracking techniques of PV system for uniform insolation and partial shading condition. *Renewable and Sustainable Energy Reviews*, *19*, 475-488.

[11] Pareek, S., & Dahiya, R. (2016). Enhanced power generation of partial shaded photovoltaic fields by forecasting the interconnection of modules. *Energy*, *95*, 561-572.

[12] Rani, B. I., Ilango, G. S., & Nagamani, C. (2013). Enhanced power generation from PV array under partial shading conditions by Shade dispersion using Su Do Ku configuration. *IEEE Transactions on sustainable energy*, *4*(3), 594-601.

[13] Potnuru, S. R., Pattabiraman, D., Ganesan, S. I., & Chilakapati, N. (2015). Positioning of PV panels for reduction in line losses and mismatch losses in PV array. *Renewable Energy*, *78*, 264-275.

[14] Chong, B. V. P., & Zhang, L. (2013). Controller design for integrated PV–converter modules under partial shading conditions. *Solar Energy*, *92*, 123-138.

[15] Sun, D., Ge, B., Peng, F. Z., Haitham, A. R., Bi, D., & Liu, Y. (2012, May). A new grid-connected PV system based on cascaded H-bridge quasi-Z source inverter. In *Industrial Electronics (ISIE), 2012 IEEE International Symposium on* (pp. 951-956). IEEE.

[16] Koutroulis, E., & Blaabjerg, F. (2012). A new technique for tracking the global maximum power point of PV arrays operating under partial-shading conditions. *IEEE Journal of Photovoltaics*, *2*(2), 184-190.

[17] Deshkar, S. N., Dhale, S. B., Mukherjee, J. S., Babu, T. S., & Rajasekar, N. (2015). Solar PV array reconfiguration under partial shading conditions for maximum power extraction using genetic algorithm. *Renewable and Sustainable Energy Reviews*, *43*, 102-110.

[18] Dhimish, M., & Holmes, V. (2016). Fault detection algorithm for grid-connected photovoltaic plants. *Solar Energy*, *137*, 236-245.

[19] Dhimish, M., Holmes, V., & Dales, M. (2016, September). Grid-connected PV virtual instrument system (GCPV-VIS) for detecting photovoltaic failure. In *Environment Friendly Energies and Applications (EFEA), 2016 4th International Symposium on* (pp. 1-6). IEEE.

[20] Chine, W., Mellit, A., Pavan, A. M., & Kalogirou, S. A. (2014). Fault detection method for grid-connected photovoltaic plants. *Renewable Energy*, *66*, 99-110.

[21] Chine, W., Mellit, A., Lughi, V., Malek, A., Sulligoi, G., & Pavan, A. M. (2016). A novel fault diagnosis technique for photovoltaic systems based on artificial neural networks. *Renewable Energy*, *90*, 501-512.

[22] Silvestre, S., da Silva, M. A., Chouder, A., Guasch, D., & Karatepe, E. (2014). New procedure for fault detection in grid connected PV systems based on the evaluation of current and voltage indicators. *Energy Conversion and Management*, *86*, 241-249.

[23] McEvoy, A., Castaner, L., & Markvart, T. (2012). Solar cells: materials, manufacture and operation. Academic Press.

[24] Sera, D., Teodorescu, R., & Rodriguez, P. (2007). PV panel model based on datasheet values. Paper presented at the 2392-2396. doi:10.1109/ISIE.2007.4374981

[25] Silvestre, S., Boronat, A., & Chouder, A. (2009). Study of bypass diodes configuration on PV modules. *Applied Energy*, *86*(9), 1632-1640.

[26] Sera, D., Teodorescu, R., & Rodriguez, P. (2008, November). Photovoltaic module diagnostics by series resistance monitoring and temperature and rated power estimation. In *Industrial Electronics, 2008. IECON 2008. 34th Annual Conference of IEEE* (pp. 2195-2199). IEEE.

[27] Spataru, S., Sera, D., Kerekes, T., & Teodorescu, R. (2015). Diagnostic method for photovoltaic systems based on light I–V measurements. *Solar Energy*, *119*, 29-44.

[28] Bastidas-Rodríguez, J. D., Franco, E., Petrone, G., Ramos-Paja, C. A., & Spagnuolo, G. (2015). Model-based degradation analysis of photovoltaic modules through series resistance estimation. *IEEE Transactions on Industrial Electronics*, *62*(11), 7256-7265.

[29] Sera, D., Mathe, L., Kerekes, T., Teodorescu, R., & Rodriguez, P. (2011, November). A low-disturbance diagnostic function integrated in the PV arrays' MPPT algorithm. In *IECON 2011-37th Annual Conference on IEEE Industrial Electronics Society* (pp. 2456-2460). IEEE.